



Flood hazard delineation in an ungauged catchment by coupling hydrologic and hydraulic models with geospatial techniques—a case study of Koraiyar basin, Tiruchirappalli City, Tamil Nadu, India

Surendar Natarajan · Nisha Radhakrishnan

Received: 29 April 2020 / Accepted: 29 September 2020 / Published online: 8 October 2020
© Springer Nature Switzerland AG 2020

Abstract Flooding in urban basins is a major natural catastrophe that leads to many casualties of life and property. The semi-urbanized Koraiyar River basin in Tamil Nadu has important cities like Tiruchirappalli and many towns located in it. The basin unfailingly experiences a flood event in almost every decade. It is anticipated that the basin will undergo rapid unplanned urbanization in the years to come. Such fast and erratic urban developments will only increase the risk of urban floods ultimately resulting in loss of human lives and extensive damages to property and infrastructure. The effects of urbanization can be quantified in the form of land use land cover (LULC) changes. The LULC change and its impacts on urban runoff are studied for the continuous 30-year present time period of (1986–2016) to reliably predict the anticipated impact in the future time period of (2026–2036). The analysis of land cover patterns over the years shows that urbanization is more prevalent in the northern part of the basin of the

chosen study area when compared with the other regions. The extreme rainfall events that occurred in the past, and the probable future LULC changes, as well as their influence on urban runoff, are studied together in the current study. In order to minimize flood damages due to these changing land use conditions, certain preventive and protective measures have to be adopted at the earliest. There are some inevitable limitations while applying traditional measures in flood modeling studies. This investigative work considers a case study on the ungauged Koraiyar floodplains. The spatial scale risk assessment is assessed by coupling geographic information systems, remote sensing, hydrologic, and hydraulic modeling, to estimate the flood hazard probabilities in the Koraiyar basin. The maximum flood flow is generated from the Hydrologic Engineering Centre-Hydrologic Modeling System (HEC-HMS), the hydrologic model adopted in the present study. The maximum flood flow is given as input to the Hydrologic Engineering Centre-River Analysis System (HEC-RAS), an effective hydraulic model that generates water depth and flood spread area in the basin. The flood depth and hazard maps are derived for 2, 5, 10, 50, and 100-year return periods. From the analysis, it is observed that the minimum flood depth is less than 1.2 m to a maximum of 4.7 m for the 100-year return period of past to predicted future years. The simulated results show that the maximum flood depth of 4.7 m with flood hazard area of 4.32% is identified as high hazard zones from the years 1986–2036, located in the center of the basin in Tiruchirappalli city. The very high hazard flood-affected zone in the Koraiyar basin during this period is about

Electronic supplementary material The online version of this article (<https://doi.org/10.1007/s10661-020-08650-2>) contains supplementary material, which is available to authorized users.

S. Natarajan (✉) · N. Radhakrishnan
Civil Engineering Department, National Institute of Technology,
Tiruchirappalli, Tiruchirappalli, Tamil Nadu 620015, India
e-mail: surendarnatarajan86@gmail.com

e-mail: 403114052@nitt.edu

N. Radhakrishnan
e-mail: nisha@nitt.edu

198.85 km². It is noticed that the very low hazard zone occupies more area in the basin for the present and future simulations of flood hazard maps. The results show that the increase in peak runoff and runoff volume is marginally varied.

Keywords Koraiyar basin · Land use land cover (LULC) · Floodplain · Flood hazard · HEC-HMS · HEC-RAS

Introduction

Flood is defined as an overflow of water that stresses the natural runoff channels (Ward 1978). Floods are a natural part of the hydrological cycle, but they can cause extensive damages to property, necessitate the sudden shifting of residents to safer areas, ruin the environment, and result in economic losses (EU Parliament Council floods directive 2007). Floods occur in coastal areas, reservoirs, and rivers when the water flow is far more than the holding scope of the natural channels (Zhang et al. 2014). In the twentieth century, nearly 1 to 14 lakh people lost their lives and were affected by catastrophic floods (Hajat et al. 2003). From various studies, it is noted that there is an increasing trend in the rate and volume of flood damages throughout the twenty-first century that have caused most severe natural disasters worldwide resulting in thousands of human casualties and extensive economic losses (Changnon et al. 2000; Ashmore and Church 2001; Alley et al. 2003; Guhasapir et al. 2004; Parry et al. 2007; Luger et al. 2010; Sahoo and Sreeja 2015; Karagiorgos et al. 2016; Abdel-Fattah et al. 2017; Koneti et al. 2018; Thirumurugan and Krishnaneni 2018; Aryal et al. 2020; Prama et al. 2020). Europe and the USA alone have reported a death toll of around 247 from 13 river flooding events. The primary causes of flood-related deaths can be classified into three types, namely physical trauma (11.7%), drowning (67.6%), and other related issues (2.8%) (Jonkman and Kelman 2005). The main reasons for flood instances are increasing number of settlements and rapid decrease in vegetation and forest cover, which result in increased runoff during excess rainfall events (UCAR 2010; Sunkpho and Ootamakorn 2011). Although floods cannot be controlled, their adverse impacts can be minimized to a large extent with the implementation of proper flood control systems. Flood forecasting is a necessary prerequisite for devising

appropriate flood control systems. It is required to determine the flow rates and water surface levels at specific points in a river system (Daniel and Mays 2015).

Flood risk reduction plans can be either structural or non-structural measures based upon the considered floodplain. The structural measures include flood retaining walls, levees, and channel diversion structures to reduce flood levels. The non-structural measures include land use management practices and standard flood modeling methods which serve as preventive measures to reduce flood risk (Ghanbarpour et al. 2014).

Flood hazard mapping is an important part of land use planning and management; it continues to be the focus of many global research studies (Chen et al. 2009a, b; Masood and Takeuchi 2012; Alfieri et al. 2014). Land use practices have been identified as one of the parameters influencing the peak runoff and volume in urban watersheds (Costae et al. 2003; Sahoo and Sreeja 2014). They are one of the primary factors responsible for increased flood risk in urban areas. LULC studies are essential in flood modeling works as it is a causative factor for the significant alteration of the urban hydrologic cycle (Melesse and Shih 2002). The hydrographs for various LULC conditions are generated by using Soil Conservation Services Curve Number techniques in the Hydrologic Engineering Centre-Hydrologic Modeling System (HEC-HMS) model for generating peak discharge in the ungauged basin (Zope et al. 2015).

Recent advances have made it possible for satellite data to be used for the accurate prediction of extent and area of floods (Jayaraman et al. 1997; Yang et al. 2006; Mai and Smedt 2017; Aryal et al. 2020). For hydrological modeling, GIS is used along with hydrologic and hydraulic models, to analyze multi-spatial and temporal data (Merwade et al. 2008; Gallegos et al. 2009). For developing any hydrologic model, digital elevation model (DEM) with GIS is used to extract essential geographical details of the basin (Tarboton and Ames 2001; Siart et al. 2009; Thirumurugan and Krishnaneni 2018).

Barranquilla is a city in Columbia (South America) frequently affected by floods due to high intensity of rainfall that overwhelms the capacity of the urban drainage systems (Melisa Acosta-Coll et al. 2018). Remote sensing techniques coupled with GIS built hydrological modeling with Quick Bird imagery were used to identify the LULC change and the flood risk areas in the Chi Minh city, Vietnam (An Thi Ngoc Dang and Lalit

Kumar 2017). Ain Sefra city located in the western part of Ksour mountains experienced flash floods during the years 1904–2007, with the worst flood event occurring in 2014. For flood modeling studies, tools like HEC-HMS, HEC-RAS, WMS, and GIS were adopted to identify the flood accumulation zones in the city (Derdour and Bouanani 2019). In Neka River basin in Northern Iran, with the active participation of residents in flood control measures, the floodplain was evaluated by the contingent valuation method (CVM) combined with hydraulic model HEC-RAS and HEC Geo-RAS for flood simulation (Ghanbarpour et al. 2014). The 2D HEC-RAS model was used to calculate hydraulic parameters such as velocity, depth, and rise rate of water to develop a regional loss of life equation in Kan watershed, Tehran, Iran (Mehdi Karbasi et al. 2018).

A flood modeling study was done for the Santa River in Peru, by using a 1D flood model with HEC-RAS. The river survey was carried out at 120 cross sections with a peak discharge of 580 m³/s. The modeling results showed good agreement with the field data of lake flood levels, wave height, and flood extent area (Jan Klimes et al. 2014). Applied methods like statistical analyses, flash flood potential index, and hydraulic modeling were used to determine flood inundation in the catchment area of the S^lanic River catchment situated in Romanian Carpathians (Zaharia et al. 2015). In Narmab dam in the east of Golestan Province of Iran, ArcView GIS was integrated with HEC-RAS to produce flood maps for determining flood discharge for different return periods (Madadi et al. 2015). In the Conestoga River located in USA, the flow rate was simulated by using Hydrologic Engineering Center (HEC)-2, and a minor correction was done in the 2013 HEC-RAS module (Weaver 2016). The 1D/2D integrated hydrodynamic modeling was used to simulate the flood inundation in low-lying areas of Surat city in India (Dhruvesh et al. 2017). In Taiwan, the analysis of climate variability with flood frequency analysis and flood mitigation measures was undertaken in the Tou-Chien River basin by using the 1D–2D numerical model (Kwan Tun Lee and Pin-Chun Huang 2018).

A 100-year flood hazard map was generated for Guwahati city in India, by measuring the flood risk and the parameters responsible for the floods. The LULC map of the city was developed for the years 2006 and 2011, and it was noted that an increase in imperviousness caused an increase in surface runoff (Sahoo and Sreeja 2015). Human-induced LULC

changes and their consequent impact were the main reasons for the increase in runoff in the Oshiwara River basin in Mumbai (Zope et al. 2016). A hydraulic model was adopted for deterministic flood forecasting in Canada, to generate a floodplain map that differentiated between flooded and non-flooded areas (Bharath and Elshorbagy 2018).

For any flood modeling, accurate boundary delineation is required, which can be done by DEM. It is used to model flood events by combining grid-formatted geospatial data with satellite data through GIS techniques, to define the relationship between flood extent, elevation, and discharge with reasonable accuracy (Smith 1997; Younghun et al. 2014; Gao et al. 2018). Precise boundary delineation was done for the Varuna River basin in Uttar Pradesh, India. The boundary of the Varuna River basin was automatically derived by coarse- and medium-resolution DEMs of SRTM-30 m, ASTER-30 m, Cartosat-30 m, ALOS Palsar-12.5 m, and Cartosat-10 m. The delineated boundary was validated with a 1 m × 1 m Google Earth image (Mallikarjun et al. 2019).

The drainage network of the Alfios River in Greece was extracted from ALOS optical and radar data, and validated with topographic maps of 1/50,000. The DSM was generated from ALOS PALSAR and ALOS PRISM to evaluate the vertical and horizontal accuracies of the basin (Nikolakopoulos et al. 2015). Multi-date RADARSAT Synthetic Aperture Radar (SAR), along with GIS, was used in Dhaka city for analyzing the extreme flood event that occurred in the year 1998. The frequency of flood and water depth were created by SAR (Dewan et al. 2006). Geospatial tools such as the Global Flood Monitoring System (GFMS) and HEC-RAS model help in analyzing floods and the extent of their influence (Neeraj et al. 2017). It is important to develop a suitable methodology to reliably predict floods in ungauged basins to safeguard cities from the detrimental impacts of floods. The frequently used method to determine the occurrence of flood and examine rainfall-runoff relationships is flooding inundation modeling (Derdour et al. 2017).

For flood inundation modeling, hydraulic parameters and morphological characteristics of the river channel like water depth, flow velocity, bank erosion, and sediment discharge are required. The hydraulic modeling calculates the required parameters, and the numeric modeling is used for simulating and predicting the river flow using the governing equations (Merritt et al. 2003;

Hassan et al. 2005; Kleinhans 2005; Wu et al. 2005; Bhuiyan et al. 2015). The HEC-HMS, HEC-RAS, and WMS integrated approach is adopted for assessing and predicting the impact of flood in watershed management practices (Arnold et al. 1998; Wheeler et al. 1999; Zhang et al. 2008; Verma et al. 2010). Flood modeling is considered to be one of the divisions in the field of hydrology, but it is difficult to use it in mixed flood-plains (Thomas et al. 2015), for non-linear hydraulic characteristics (Sarhadi et al. 2012) and for places with uncertainty of rainfall input data (Yu et al. 2015). There are numerous hydrodynamic models available for 1D, 2D, and 1D/2D coupled hydrodynamic modeling which are used for simulating varying flood occurrences (Quiroga et al. 2016). Numerical models are essential tools for a better understanding of the magnitude of extreme flood events and assessment of similar other hazards (Salimi et al. 2008).

According to Price and Vojinovic (2008), flood risks can be minimized by circulating beforehand among the public, flood risk maps that clearly depict the locations that face imminent danger of floods. Flood maps can be divided into two important categories, namely, flood hazard maps and floodplain maps (Stevens and Hanschka 2014). Flood hazard maps give information on individual flood-affected localities, areas that fall under flood risk, and the parameters that cause flood events. Flood hazard maps are important, as they take into consideration the influence of all the parameters responsible for floods. The coupling of GIS and remote sensing with hydrological and hydraulic models offers a valuable tool for assessing the impact of LULC on surface runoff, spatially as well as temporally (Hathout 2002; Herold et al. 2003; Lambin et al. 2003; Serra et al. 2008; Dewan and Yamaguchi 2009). In their studies, Zope et al. (2015, 2016 and 2017) discussed LULC changes and their effect on floods in Poisar, Oshiwara basin (Mumbai). Flood modeling studies were done for past and present changing LULC conditions. The only limitation of their study was that future LULC changes and flood risk maps were not taken into consideration.

Identification of novelty from literature review

From the comprehensive review of literature, it is noted that very few flood modeling studies have been carried out related to urban flood modeling with emphasis on future flood prediction in a medium-size urban catchment area. Therefore, an integrated modeling approach

is adopted in this study of an ungauged basin, and various changes in LULC as well as their impact on the urban basin are investigated. To the best of the author's knowledge, this is the first flood modeling work to be undertaken for the chosen study area of Koraiyar basin. The uniqueness of this study is that future prediction of flood modeling is also done. The developed model will also be useful for assessing other ungauged basins with similar conditions.

Objectives of the study

The present research study aims

- To apply hydrological and hydraulic models in the Koraiyar River basin along with geospatial techniques for generating a conceptual flood model.
- To create a 2D model for the Koraiyar basin by using HEC-RAS 5.0.7.
- To simulate the flood scenario for changing LULC classes in the basin for past, present, and future conditions.
- To generate floodplain and flood hazard maps of the Koraiyar basin to identify the areas in the basin prone to high risk of flooding, and to propose suitable precautionary measures to reduce the adverse impacts of floods.

Study area description

The Koraiyar River and its catchment lie between the latitude of 10° 32' 40.24" N and 10° 48' 16.81" N and longitude of 78° 32' 23.94" E and 78° 39' 48.58" E in Tiruchirappalli city, South India. It originates from the Othakkadai Karupur Redipatti hills in Manaparai taluk of Tiruchirappalli district and finally flows into Uyyokondan channel in the center of Tiruchirappalli city, Tamil Nadu, as shown in (Fig. 1). The river basin has a subtropical climate. There is no significant temperature difference between summer and winter, with summer (March to May) having an extreme temperature of 41 °C and a least of 36 °C; winter (December to February) is generally warm but pleasant with temperatures ranging from 19 to 22 °C.

Hot, humid, dry summers and mild winters are the main climatic features of the basin. The rainy season that falls between October and December brings rain mostly from the northeast monsoon. The river flows through

Manaparai, Thuvankurichi, and Viralimalai, and the total length of the main river is 75 km, with a catchment area of 1498 km². The average annual rainfall for the Koraiyar urban catchment is around 757.40 to 866.70 mm. The surplus water flows through Puthur weir outlet in the left bank of the Uyyakondan River and traverses Kodamurutty River for a length of 6 km before finally falling into the Bay of Bengal. The rain gauge station for the Koraiyar basin is located at Trichy Airport. The Koraiyar River, passing through Tiruchirappalli city with an area of 167.23 km², has experienced frequent floods in the years 1924, 1952, 1954, 1965, 1977, 1979, 1983, 1999, 2000, and 2005. An interaction with the PWD Engineer reveals that the 1999 flood event had resulted in huge loss of human lives, agriculture, and property compared with many other rainfall events. Therefore, the 1999 extreme rainfall event is considered as a benchmark for developing floodplain and flood hazard maps.

Research methodology adopted in the study

Methodology framework

The research strategy adopted to conduct the current study is shown in (Fig. 2). The methodology involves data collection, hydraulic software selection, and analysis. The processing of gathered hydrologic and hydraulic data for generating floodplain and flood hazard maps is stated in detail.

Data generation

The DEM data of 30-m resolution is used in this study, as shown in (Fig. 3), downloaded from Advanced Land Observing Satellite (ALOS) developed by the Japan Aerospace Exploration which automatically extracts drainage networks and catchments based on geometric data for the basin (Nikolakopoulos et al. 2015). The geometric data, such as river centerline, banks, flow path, and cut lines, is generated using HEC-GeoRAS software. The triangulated irregular network (TIN) is used to obtain the attributes of the spatial geometric data. The predicted flood flow simulated from the hydrologic model (HEC-HMS) is given as input to the HEC-RAS. The water surface profile and its spread generated from the HEC-RAS model are given as input for post-processing in the HEC-GeoRAS model, which is an extension of ArcGIS. The floodplain maps are

generated as the output, and they are given as input for the generation of flood hazard maps.

Developing precipitation IDF curves

The rainfall data is collected for the time period of (1977–2016) from Tiruchirappalli Airport located in the Koraiyar basin. The annual maximum extracted daily precipitation records are used for modeling and for frequency distribution analysis in the basin. The collected daily rainfall data is converted into hourly rainfall data by IMD (Indian meteorological method) and statistically analyzed by different distribution techniques. The trends of precipitation are analyzed, and the intensity of precipitation is calculated for different storm durations of 1, 3, 6, 9, 12, 15, 18, 21, and 24 h of return periods of 2, 5, 10, 50, and 100 years. The rainfall data is then analyzed to establish intensity–duration–frequency curves (IDF curves) based on the extreme value of rainfall received during this period and the basin response to the extreme rainfall event. The statistical methods of (Gumbel, log Pearson type III and log normal) distributions are employed in flood frequency analysis. The frequency cumulative distribution functions of general extreme value (GEV) are given by (μ, σ, ζ) distribution, for $\zeta \neq 0$, as shown in (Eq. 1) below,

$$F(x) = \exp\left\{-1 + \zeta\left(\frac{x-\mu}{\sigma}\right) - \frac{1}{\zeta}\right\} \tag{1}$$

where μ , σ , and ζ are the location, scale, and shape parameters, respectively (Cheng et al. 2014). Here, $F(x)$ is defined for $1 + \zeta\left(\frac{x-\mu}{\sigma}\right) > 0$ or $F(x)$ is either 0 or 1. For $\zeta = 0$, $\zeta > 0$ and $\zeta < 0$ leads to Gumbel, log Pearson type III and log normal distributions, respectively. For determining non-stationarity and significant trends in extreme precipitation events, the location parameter of the GEV distribution is allowed to be time-dependent following (Eq. 2)

$$\mu(t) = \mu_1 t + \mu_0 \tag{2}$$

where t is time and $\mu_1 t$ and μ_0 are the respective intercept and slope parameters of the linear model for the GEV location parameter as a function of time.

Development of hydrologic modeling for the basin

The data from the HEC-GeoHMS model is imported into HEC-HMS to generate peak discharge hydrographs

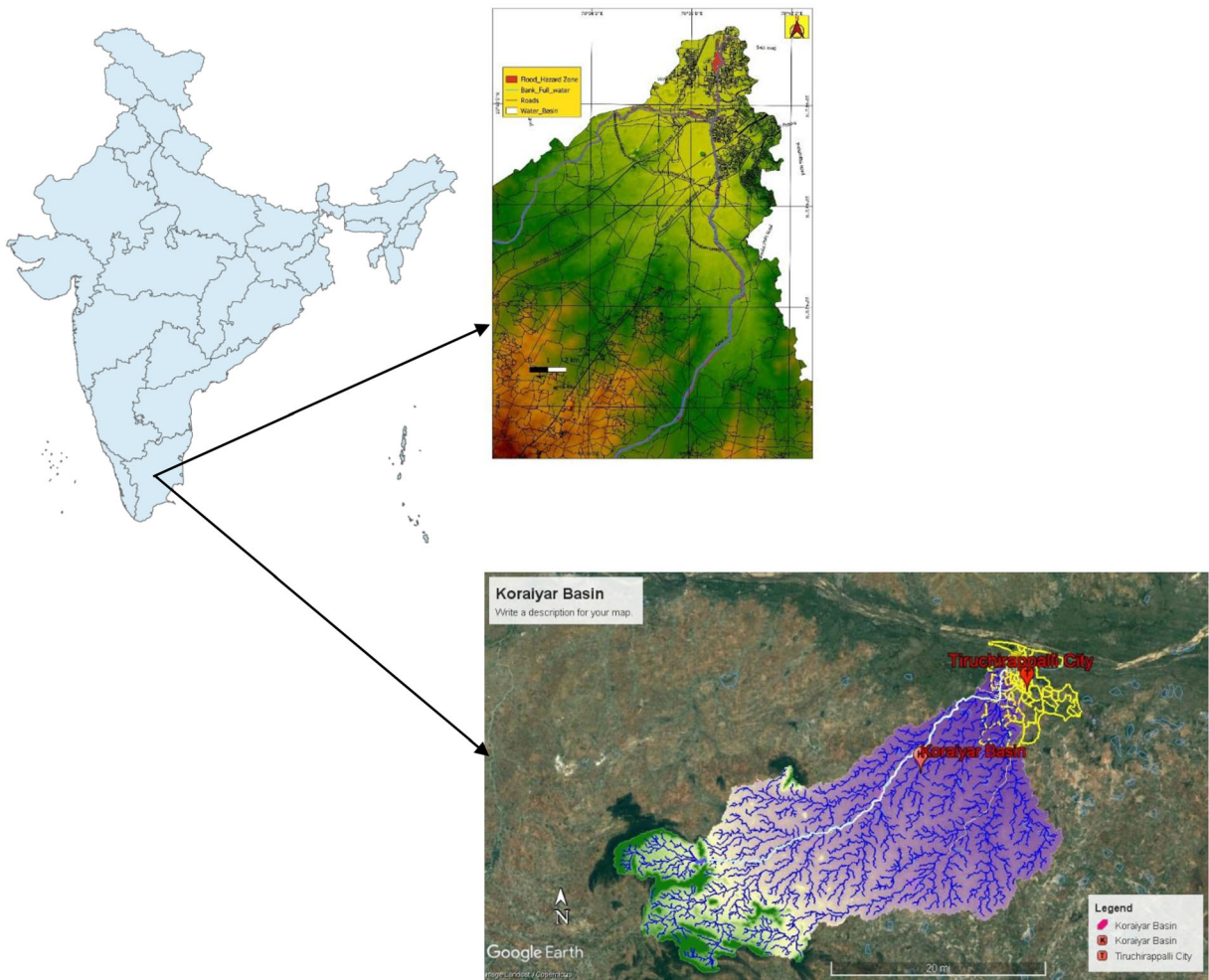


Fig. 1 Location map of the study area

at the outlet of the basin. The frequency storm method is used for estimating the flood flow in the basin for various return periods. The loss and runoff rate in the basin are calculated by the Soil Conservation Services-Curve Number (SCS-CN) and unit hydrograph method, respectively. The calibrated HEC-HMS model is used to calculate the peak flood flow for the ungauged Koraiyar River basin for the different return periods of (2, 5, 10, 50, and 100 years) and Nash–Sutcliffe efficiency (NSE) is used to validate the model’s performance and determine the goodness of fit of the statistical model.

Development of hydraulic modeling for the Koraiyar basin

HEC-RAS software, developed by the US Army Corps of Engineers (USACE 2016), is an open-source

software that can perform 1D and 2D hydraulic calculations. The basic equations that describe the one-dimensional unsteady flow are the Saint-Venant equations, represented by the continuity equation (Eq. 3) and the momentum equation (Eq. 4) (Chow et al. 1988). The continuity equation is given below:

$$\frac{\partial Q}{\partial x} + \frac{\partial A}{\partial t} - q = 0 \tag{3}$$

In terms of the momentum equation, it is stated as

$$\frac{\partial Q}{\partial t} + \frac{\partial \left(\frac{\beta Q^2}{A} \right)}{\partial x} + gA \left(\frac{\partial h}{\partial x} + S_f + S_e \right) \tag{4}$$

where x is the longitudinal distance alongside channel, t is the time, Q is the flow rate, q is lateral inflow, β is the momentum correction factor, A is

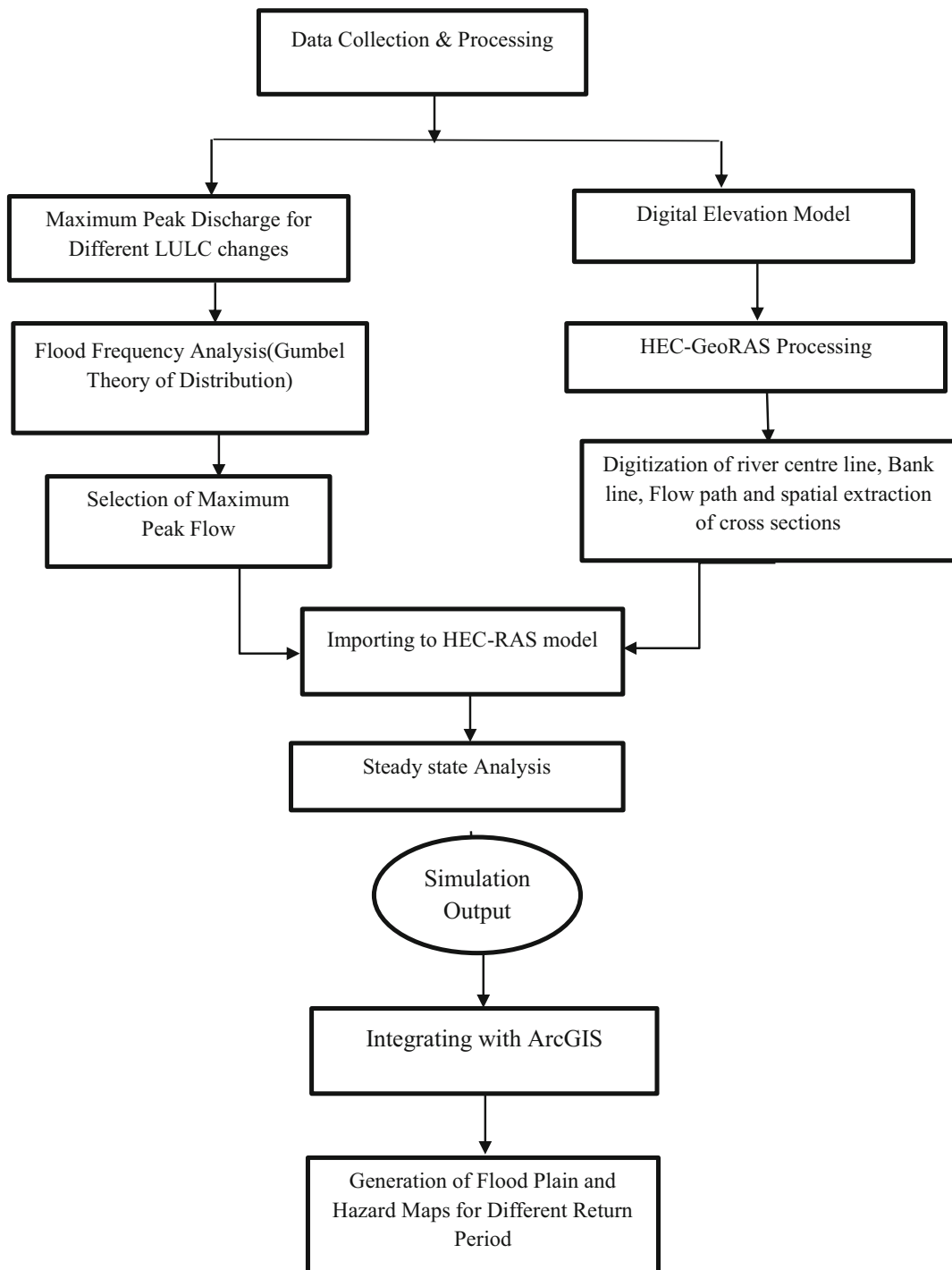


Fig. 2 Methodology framework of the study

the cross-sectional area of flow, V_x is the velocity of lateral inflow in x -direction, h is the water surface elevation in the channel, S_f is the slope of the energy grade line, S_e is the large-scale eddy loss slope for

contraction/expansion, and g is the acceleration of gravity.

For developing the hydraulic modeling, the flood flow from the hydrologic modeling is taken as input

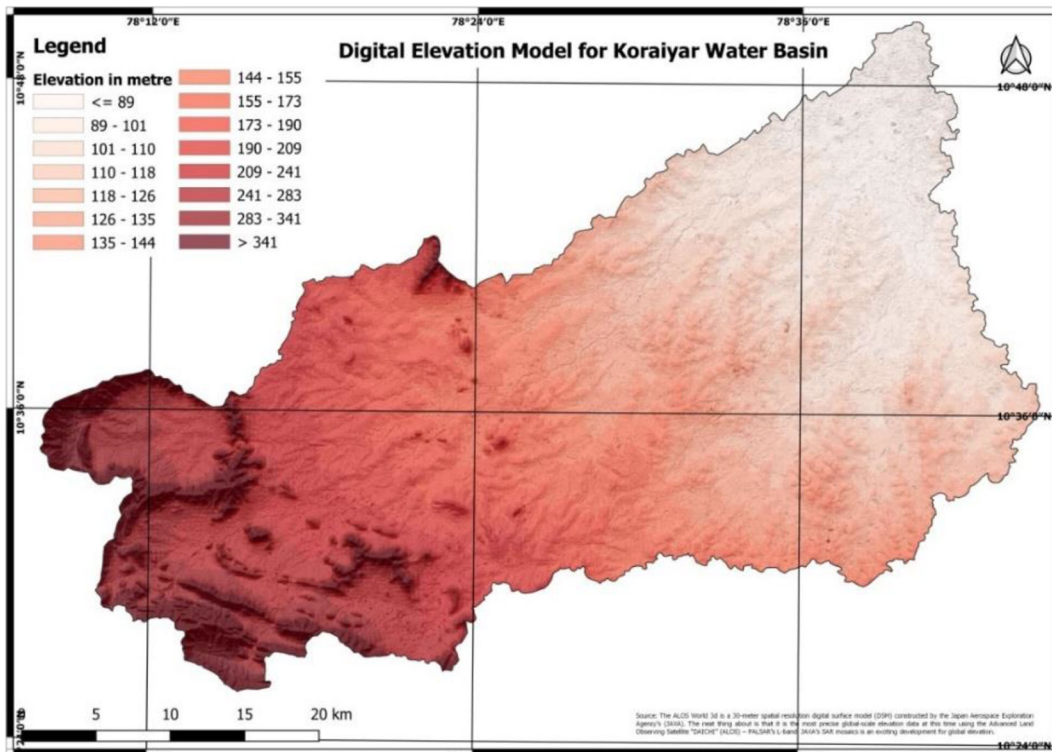


Fig. 3 Digital elevation model for the basin

for generating the flood spread. The other parameters required for generating hydraulic models are cross sections for the river basin, left and right bank locations, and roughness coefficient (Manning's constant " n " contraction and expansion constants). The roughness coefficient is estimated combining land use data with Manning's constant. The HEC-RAS version 5.0.7 is used for calculating steady flow water surface profiles. Other tools, like inundation mapping tools, are also present in this hydraulic model. The flood peak for different return periods of 2, 5, 10, 50, and 100 years is considered. The discharges of the different return periods are calculated.

One-dimensional hydraulic modeling

The sequential steps for generating the 1D hydraulic modeling are as follows:

1. The sub-basin and geometric data of the river basin are prepared from ArcGIS extension, HEC-GeoHMS, and HEC-GeoRAS, as shown in Fig. 4. A total number of 27 sub-basins are created through HEC-GeoHMS process.

2. The steady flow analysis is performed by identifying the values of upper and lower boundary conditions in the river stream area to be modeled.
3. The maximum flood flow discharge is adopted as the upstream boundary condition and uniform streamflow as the lower stream boundary condition. The parameters like energy line, slope, stream bed, and water level are adopted for modeling purposes.
4. The results for the HEC-RAS are extracted from HEC-GeoRAS.
5. The water surface profiles are generated for each cross section, and a surface model is generated for water levels in TIN format.
6. Finally, water depths are generated in raster format for individual cross sections.

Cross sections of the Koraiyar basin

An aggregate of 60 cross sections is taken for the Koraiyar River basin through spatial data processing in HEC-GeoRAS, as shown in Fig. 5. The cross sections are used as one of the parameters for generating

floodplain maps. The roughness coefficient for each cross section of the basin is assigned based upon different LULC cover classes, as shown in Table 1 (Chow 1959).

Hydraulic modeling for the Koraiyar basin

Hydraulic modeling is used to obtain floodplain and flood hazard maps for the Koraiyar basin in Tiruchirappalli city. The hydrologic model is used to determine the flood flow for each catchment, and it is given as input to the hydraulic model HEC-RAS for generating the flood depths in 2D for the different return periods of various LULC for the present period (1986–2016) and predicting future trends (2026–2036). The flood depth and its spread are defined through cross sections extracted through the spatial approach in the basin. The distance between each cross section is 110 m with the width of 400 m. The river stations are fixed as it is necessary for delineating the hydraulic process in each cross section based on the distance. The Koraiyar River starts at section number 41,914.20 and ends at 16,201.3 section in the basin, as shown in Fig. S1. During the year 1986, the maximum peak discharge is obtained at station number 35,864.05 for the 5-year return period. Further flood spread is noted at the downstream cross-sectional number 207,001.3 for the 10-year return period. Similarly, it is seen that the downstream stations of 13,651.33 and 16,201.33 experienced high flood depth for 50 and 100-year return periods. In the years 1996 and 2006, an increase in flood depth is observed at station 29,314,054. Peak flow is observed in the year 2016 at station 29,551.53. In a similar manner, a flood rise is forecasted for the years 2026 and 2036 in the 21,364.2, 28,414.20, and 1943.769 stations.

The roughness coefficients are assigned for each cross section delineated from the basin. The roughness coefficients used in the study area are 0.060 for vegetation, 0.150 for forest areas, 0.020 for settlement areas, 0.035 for waterbodies, 0.05 for agricultural land, and 0.040 for open land. A mixed condition of flow is chosen for the HEC-RAS. The upstream boundary condition is set as a critical depth, while the downstream end is considered as normal depth. Once all the input data and boundary conditions in HEC-RAS are met, the simulation is carried out as a steady-state analysis. The flood hazard maps are generated by keeping the extreme event of rainfall as a constant factor for different LULC for the years 1986, 1996, 2006, 2016, 2026, and 2036.

Results and discussion

Analysis of rainfall data

The Gumbel extreme value distribution is used since it produces better and more accurate results when compared with the other two methods (Surendar and Nisha 2019a). The Gumbel method is used due to its skewness and its accuracy in data distribution. The generated IDF curve is plotted on a normal scale for Gumbel distribution method for $T_r = 2, 5, 10, 50,$ and 100 years, as shown in Fig. 6. From the modeled IDF curve, it is observed that for the 100-year period, the rainfall intensity in the Koraiyar basin is 11.1 mm/h. For the 10 and 50-year return periods, the rainfall intensity is between 6.86 and 9.84 mm. For the design of an appropriate drainage system, the 2 and 5-year return periods can be used. In this study, the entire basin is assumed to receive an identical amount of rainfall. The extreme rainfall event that occurred on 22 November 1999 is used for estimating the peak discharge from the basin for different intervals (Surendar and Nisha 2019b). The employment of this statistical method allows the estimation of peak discharges for different average return periods.

The extreme rainfall event in the basin ranges between 101.90 and 310.55 mm/day over the considered past 40 years. Rainfall values from 124.5 to 224.4 mm are considered as extreme rainfall event, as per IMD (India Meteorological Department) (Rajeevan and Bhate 2008). Flood is said to have occurred when there is precipitation of more than 100 mm within a short duration of heavy rainfall (Gaume et al. 2009). In the present study, rainfall values of more than 100 mm are considered for runoff generation, but only one selected extreme precipitation event of 310.55 mm is considered for generating the floodplain and flood hazard maps. This study primarily concentrates on the selected extreme rainfall event and focuses on LULC change and its impact on surface runoff.

The extreme rainfall event is selected for simulating the flood flows for the return periods of 2, 5, 10, 50, and 100 years, as shown in Table 2. The simulated values of various return periods during the extreme rainfall event that occurred on 22 November 1999 show that the peak discharge and volume for the Koraiyar basin for a return period of 100 years are 570.3 m³/s and 11.74 mm, respectively. Similarly, for the other return periods of 2, 5, 10, and 50 years, the peak discharge and volume

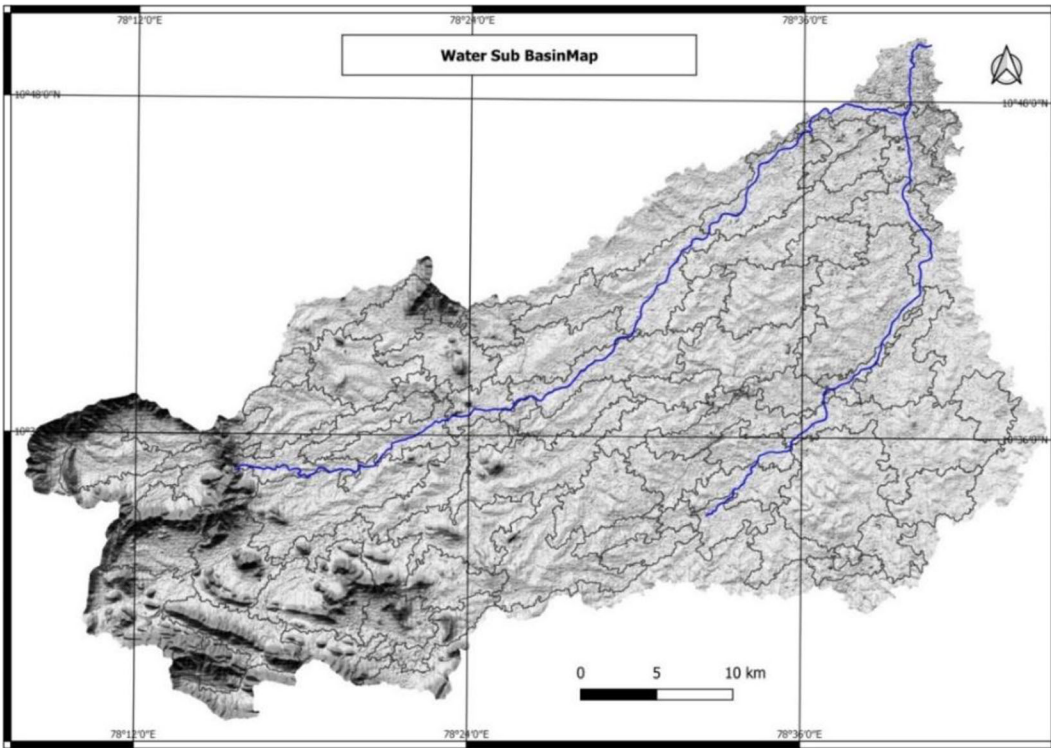


Fig. 4 Sub-basin and geometric data of the Koraiyar River basin extracted from HEC-Geo HMS and HEC-Geo RAS

are 500.4 m³/s, 320.6 m³/s, 118.2 m³/s, and 102.2 m³/s and 2.7 mm, 3.2 mm, and 6.72 mm, respectively. The differences between observed and simulated values are tested with NSE values. The obtained NSE coefficient

of 0.45 to 0.73 proves that the hydrological modeling results are satisfactory. The results obtained are acceptable and can be considered for simulation of the rainfall-runoff model (Moriassi et al. 2007).

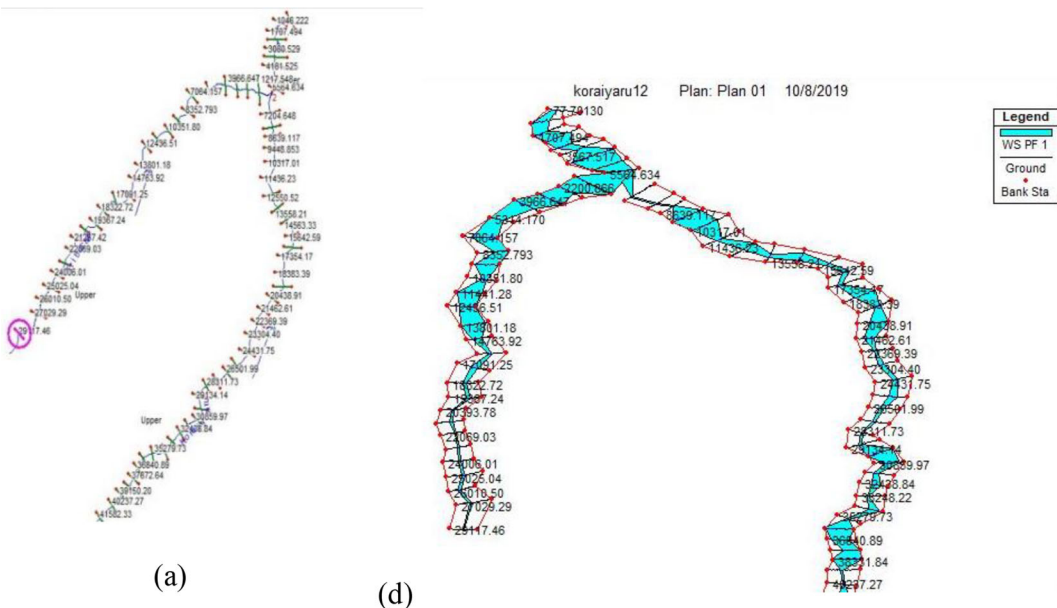


Fig. 5 HEC-RAS geometry for the Koraiyar basin. **a** Cutlines. **b** x–y–z perspective plot

Table 1 Manning’s roughness coefficient for different LULC classes (Chow 1959)

Land use land cover	Manning’s roughness coefficient
Open land	0.040
Vegetation	0.045
Forest	0.4
Settlement	0.06
Agriculture	0.05
Water bodies	0.035

LULC changes

The LULC change is the main reason for flooding in the urban region due to changes in the urban hydrological process (Chen et al. 2009a, b). In this study, the LULC changes from 1986 to 2016 are analyzed and the future prediction is also studied, as mentioned in the methodology. The LULC classes considered for this study are open land, vegetation, forest areas, settlement areas, agricultural land, and waterbodies.

The LULC maps for the basin developed in an earlier study by the authors for the years 1986–2016 are shown in (Fig. S2); they are also generated for the future, i.e., the years 2026 and 2036. The percentage of LULC clearly shows that there is a change in LULC between 1986 and 2016, as shown in Table 3. From the results, it is noticed that there is an increase of 104.74% in the settlement area, and a decrease of 11.45% and 12.29% in the number of waterbodies and agricultural land, respectively, during this period. The Markov model, along with GIS, measures the future trend of LULC changes for the years 2026 and 2036. The simulated results show there is an overall increase of 7.17% in the

settlement area from 1986 to 2036. From the analysis, it is detected that the LULC has undergone significant changes in the past and is also very likely to undergo further changes in the future. The soil map, along with LULC maps and the curve number (CN), are generated for the Koraiyar River basin (Surendar and Nisha 2019b). The generated CN clearly shows that there is an increase in CN values from the past to the future. The increase in CN proves the increase in peak runoff and runoff volume.

Effect of LULC changes on peak flood flow

In this study, the LULC change and its effect on surface runoff are analyzed for the rainfall depths of different return periods for the land use conditions of the years 1986, 1996, 2006, 2016, 2026, and 2036. The surface runoff is calculated using the SCS-CN loss method in the hydrologic HEC-HMS model. The composite CN is obtained for each sub-basin and is given as input to the SCS-CN modeling in HEC-HMS (Surendar and Nisha 2019b).

From the calculated rainfall and the LULC data of 1986–2036, the runoff of the Koraiyar basin is calculated for the chosen study period. The runoff constitutes the function of rainfall intensity distribution of the year 1999 and the land use data of 1986–2036. From the analysis, it is observed that for the 2-year return period, the total runoff of the year 1986 is 43.86 m³/s, and the total runoff of the year 1996 is 42.69 m³/s. The impact factor of LULC changes for the 2-year return period is 0.973. This is used as a deciding factor for measuring the effects of LULC on the surface runoff in the Koraiyar basin, and similarly the land use impact factor

Fig. 6 Intensity–duration–frequency curves for the Koraiyar basin

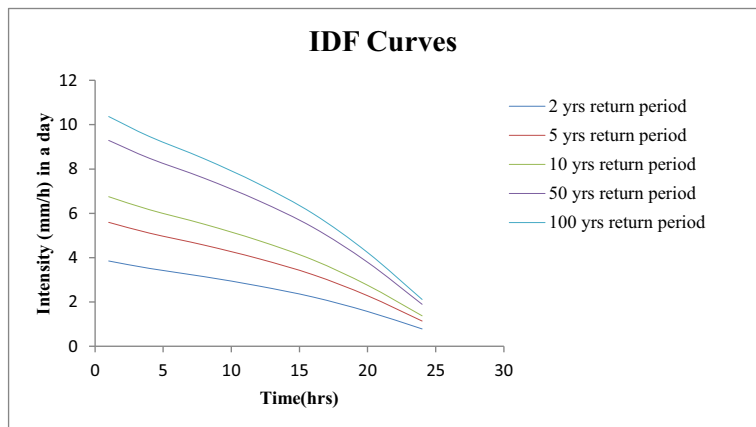


Table 2 Simulated and observed peak flow for the single extreme rainfall event that occurred in the Koraiyar basin

Single extreme event date and rainfall (mm)	Return period in years	Peak flow (m ³ /s)		Volume (mm)		NSE values
		Simulated	Observed	Simulated	Observed	
22 November 1999						
and 310.55	100	570.3	481.9	11.74	10.97	0.45
	50	500.4	420.5	10.58	9.54	0.5
	10	320.6	276	6.72	6.17	0.7
	5	118.2	205.9	3.16	4.64	0.71
	2	102.2	104.7	2.7	2.33	0.73

for the other return periods. The maximum impact factor is observed during 2016–2026 for the 100-year return period, and the minimum impact factor is observed during the 2-year return period in the year 1986. In spite of increase in urban areas, there is no proper interconnected drainage facilities like storm water network in the basin. Bushes and weeds observed along the bank of the river impede the water flow which is another reason for repeated occurrence of increased flooding in the Koraiyar River basin.

Calibration of hydraulic modeling

Model calibration and validation are essential aspects of hydraulic simulations. The calibration of the hydraulic model is not done due to lack of data and absence of a gauging station in the basin. The data used in this study is based on geoprocessing with accuracy. The flood flow in the hydraulic model is adopted based upon the flow generated from the hydrologic model. Calibration of the model is usually achieved by adapting the Manning coefficients, as already mentioned in the methodology of the study. The results of the simulation are in

Table 3 LULC change in the categorized classes of the Koraiyar basin

S. no	Land use	Area (km ²)		Change (%)
		1986	2016	
1	Openland	381.88	399.56	4.63
2	Vegetation	32.8	53.82	64.09
3	Forest	51.48	29.4	-42.89
4	Settlement	93.09	190.59	104.74
5	Agriculture	792.07	694.72	-12.29
6	Waterbody	147.01	130.18	-11.45

agreement with the information collected from the River Conservation Centre, Tiruchirappalli.

Generation of floodplain maps

Floodplain maps of the study area are developed for the years 1986, 1996, 2006, 2016, 2026, and 2036 for various LULC classes. The floodplain maps for the basin are obtained through modeling the land use conditions for 2, 5, 10, 50, and 100-year return periods' rainfall depths. The areal extent of the flood water spread for the basin area is shown in Table 4.

For the land use condition of the year 1986, the floodplain area of the sub-basin is 20.09 km² for the 2-year return period, and 41.16 km² for the 100-year return period. For the land use conditions of the year 1996, the floodplain area of the sub-basin is 20.31 km² for the 2-year return period and 41.63 km² for the 100-year return period. For the 5, 10, 50-year return periods, the flood spread is 1.44, 2.16, and 2.66 km², respectively. There is an increase in floodplains when compared with the previous year 1986. In the years 2006 and 2016, there is a marginal decrease in the floodplains for the 2-year return period when compared with the previous year 1996. Similarly, for all the other return periods, there is a slight decrease in the flood extent. The slight decrease is due to land use factors such as increase in open land, vegetation, environmental factors, and soil conditions during these years which must also be taken into consideration.

In predicting the flood extent for the future LULC of the years 2026 and 2036, it is observed that compared with the previous decades, there is a gradual increase in the floodplains for all the return periods except for the 10-year return period. In the year 2016, it is noted that for the 10-year return period, there is a marginal increase in flood spread when compared with previous years.

Table 4 Floodplain areas for different LULC and return periods

Return period years	Flood plain area (km ²)					
	LULC 1986	LULC 1996	LULC 2006	LULC 2016	LULC 2026	LULC 2036
2	20.09	20.31	20.09	19.60	20.41	20.87
5	21.35	21.56	21.35	20.52	21.64	21.93
10	32.10	32.35	32.10	30.02	32.79	33.64
50	39.41	39.88	39.41	37.48	40.18	40.92
100	41.16	41.63	41.15	39.22	42.08	42.88

The decrease in the lower return period is due to minor alteration in the physiography features of the basin. The marginal increase in the lower return period when compared with future years indicates that the flood inundation area is higher in the downstream part compared with the upstream part of the basin. The minimum and maximum flood depths expected during these years are 1.21 to 4.7 m, respectively.

From Fig. 7 depicting the 2–100-year return periods of the year 1986, it is noted that the maximum expected flood is 2.90–3.76 m. The increase in 0.86 m is expected for the 100-year return period. In the year 1996, the anticipated flood for 2–100-year return periods is 2.90–3.73 m; as shown in Fig. S3, an increase of 0.83 m is observed. Compared with 1986, a decrease of 0.03 m is noted which is mainly due to increase in open land. The predicted maximum flood for 2–100-year return periods for the year 2006 is shown in Fig. S4. A maximum flood depth of 2.90–3.63 m with an increase of 0.73 m is noted. Compared with previous years of 1986–1996, a decrease of flood depth is found because of desilting work in the river after the 2005 floods. The return periods of 2–100-year floods for the year 2016, as seen in Fig. 8, show that the maximum flood depth of 2.87–3.63 m with an increase of 0.76 m difference is seen mainly due to urbanization, and dumping of solid waste in the river. From the simulated years of 2026–2036, as seen in Figs. S5 and 9, it is observed that the maximum flood depth is 2.82–2.92 m for the 2-year return period. The flood depth of 3.78–3.81 m is noted for the 100-year return period. This increase in flood depth is mainly due to continual expansion of settlement areas and the developmental activities in nearby basin areas.

The percentage of flood inundation changes observed from 1986 to 2016 for the present and future

LULC conditions of the years 2026 and 2036 is shown in Table 5. There is a marginal decrease in the percentage of flood inundation area from 1996 to 2006 and 2006–2016 due to changes in the physiographic features, land use patterns, and weather patterns of the basin during this period of the study.

Table 6 shows that the percentage of difference in floodplain area for different LULC between the years 1986 and 2036 for 10 and 100-year return periods is 4.80% and 4.18%, respectively. The results generated show that the flood inundation area is higher for the LULC condition of 2036 as compared with 1986. From the results, it is observed that the change in percentage of the flood extent area between 1986 and 2036 for the lower return periods is less when compared with higher return periods. This is due to the fact that the downstream part of the catchment is more vulnerable than the upstream area.

The other notable reasons are as follows:

1. During extreme precipitation times of monsoon season, the flood flow from the upstream side of the river combines with downstream urban runoff leading to flood in the downstream side.
2. The flat terrain basin is also a reason for flood vulnerability in the downstream portion of the basin.
3. The water logging problems in the basin are also responsible for the flood mainly due to dumping of waste in the banks of the river near Tiruchirappalli city.
4. The storm water drains are designed for the flood discharging capacity of the past and are unable to carry the present increased flow due to increased imperviousness in the basin.

The following observations are made from the analytical study:

1. The area with higher depth is more immersed when compared with lower depth in terms of increase in flood intensity.
2. In the basin, some areas get flooded even with normal rainfall of the 2-year return period due to increase in imperviousness and flow obstruction. The flood depth exceeding 4.7 m in the 100-year return period affects a greater area when compared with the 50-year return period.

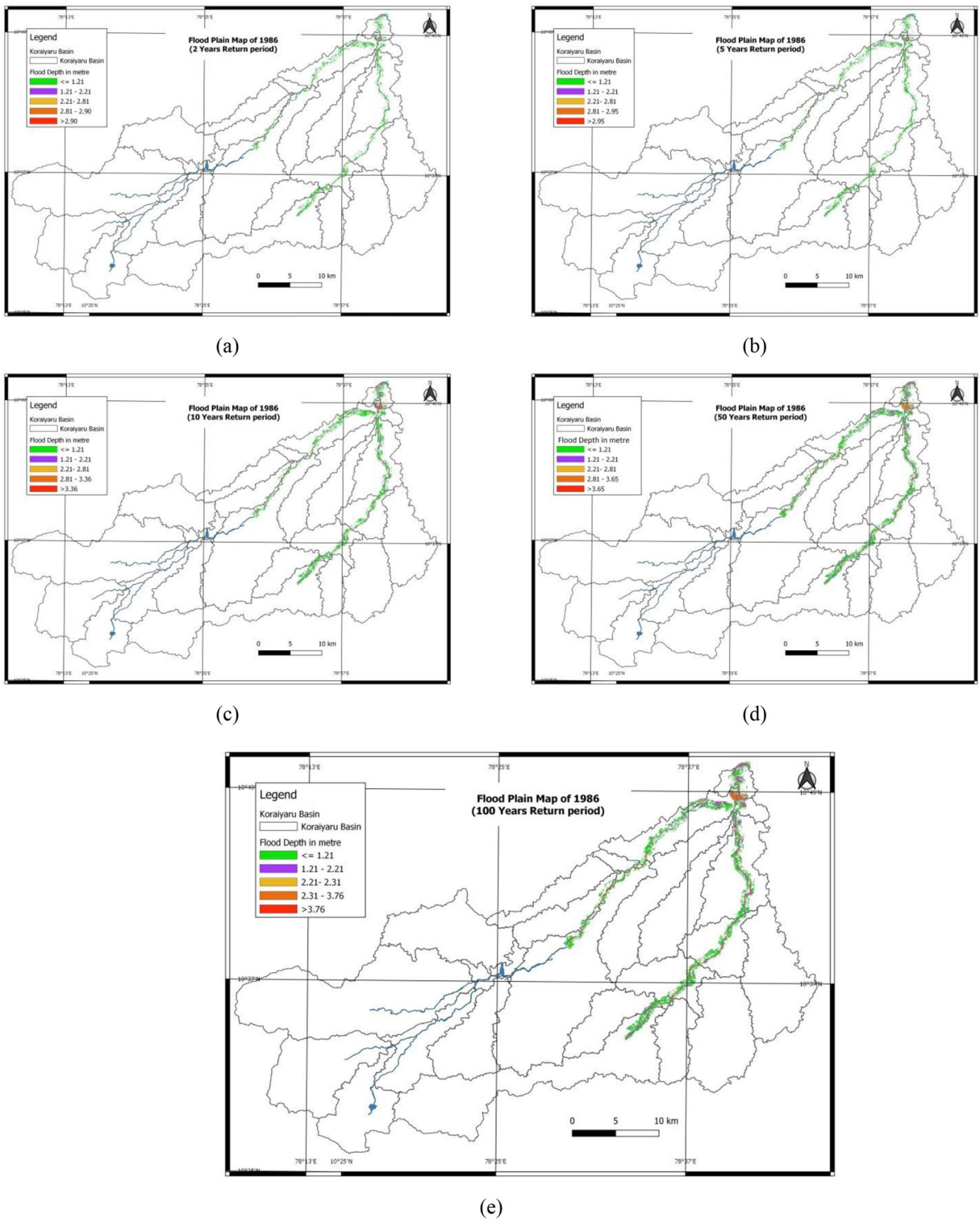


Fig. 7 Flood water depths simulated for various return periods of the year 1986 by HEC-RAS model: **a** 2, **b** 5, **c** 10, **d** 50, and **e** 100 years

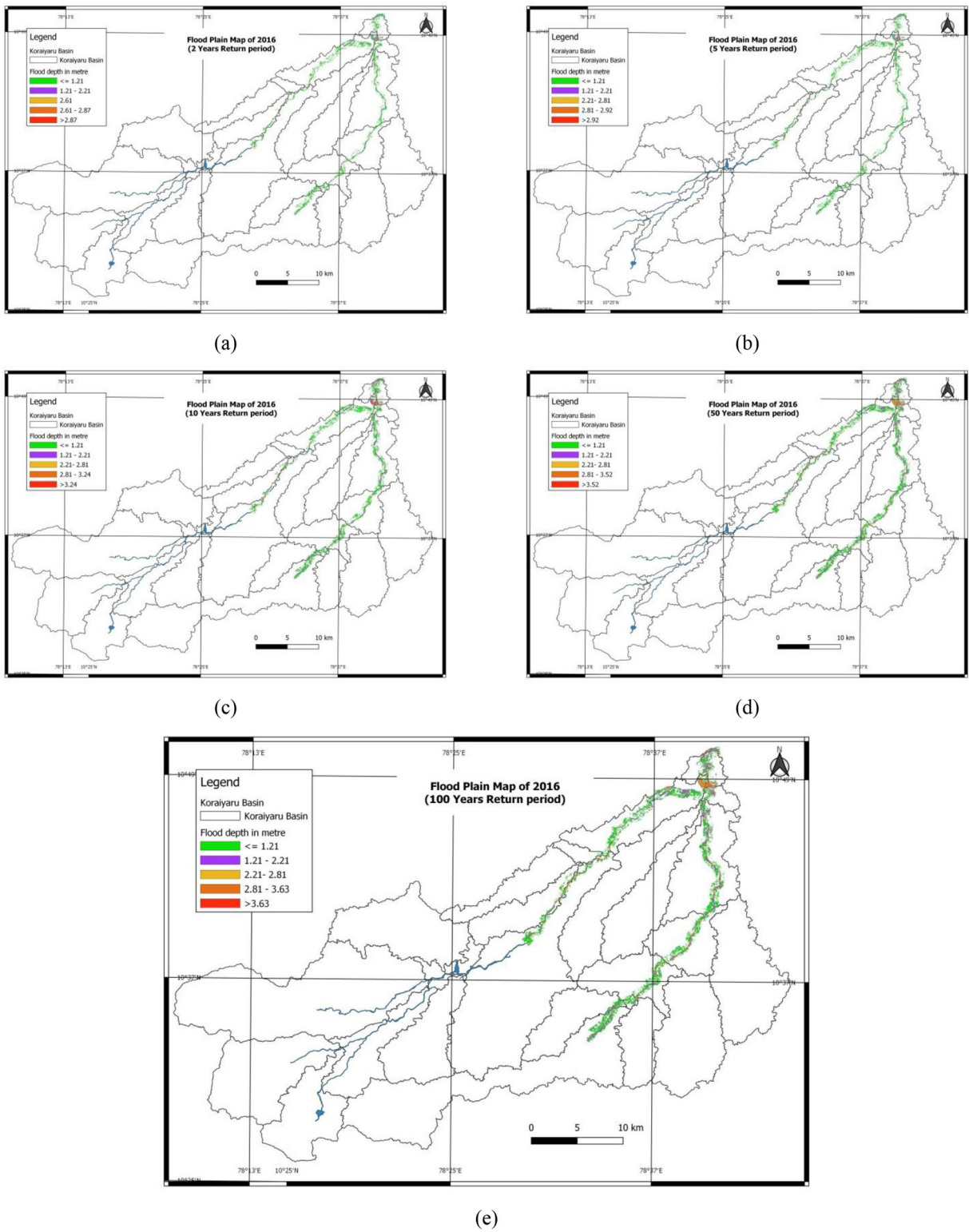


Fig. 8 Flood water depths simulated for various return periods of year 2016 by HEC-RAS model: a 2, b 5, c 10, d 50, and e 100 years

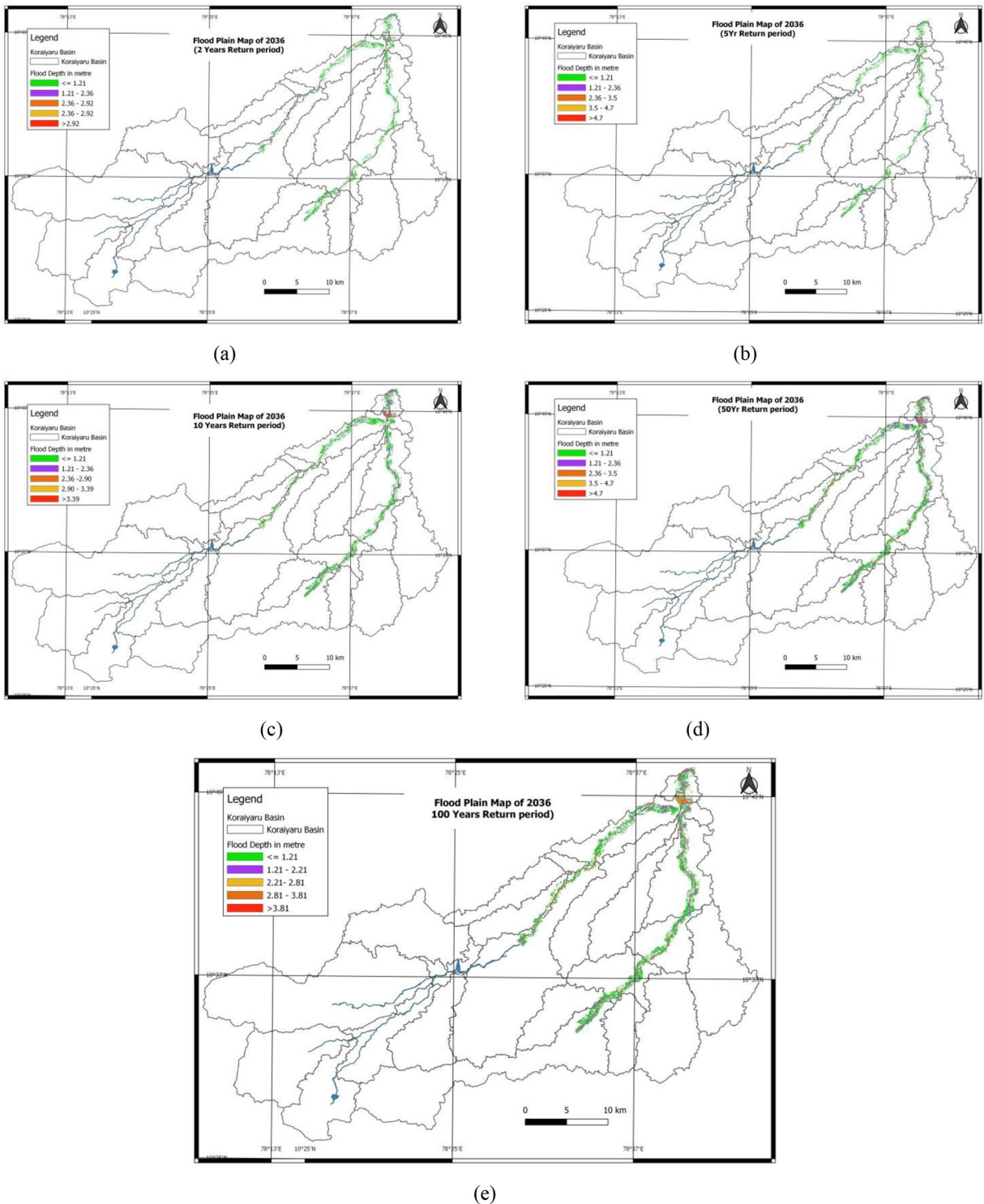


Fig. 9 Flood water depths predicted for various return periods of the future year 2036 by HEC-RAS model: **a** 2, **b** 5, **c** 10, **d** 50, and **e** 100 years

Table 5 Flood inundation changes for different LULC and return periods

Return period years	Flood plain area of sub-basin (%)					
	LULC 1986	LULC 1996	LULC 2006	LULC 2016	LULC 2026	LULC 2036
2	1.34	1.36	1.34	1.31	1.36	1.39
5	1.43	1.44	1.42	1.37	1.44	1.46
10	2.14	2.16	2.14	2.00	2.19	2.25
50	2.63	2.66	2.63	2.50	2.68	2.73
100	2.75	2.78	2.75	2.62	2.81	2.86

- The floodplain assessment confirms that the highest percentage of vulnerability in the downstream region of the Koraiyar River basin is the settlement area, followed by agricultural and open lands. Only a negligible forest area is inundated, as it is situated close to the river basin.
- The urban portions of Tiruchirappalli city located along the banks of the Koraiyar River are at a high risk of flooding due to surface runoff during the monsoon season.
- Prolonged rainfall increases the water levels which reach up to 4.7 m in the river channel passing through the city, and the inundated area affects the lives of people residing near the Koraiyar River channel.
- From the developed simulated maps of 2026–2036, it is evident that more urban areas are likely to be inundated in future and high flood hazard is predicted for the study area.

Table 6 Percentage of difference in floodplain area for different LULC and return periods

Return period years	Percentage of change in flood plain area					
	1986–1996	1996–2006	2006–2016	2016–2026	2026–2036	1986–2036
2	1.09	−1.08	−2.42	4.13	2.23	3.87
5	0.99	−0.98	−3.89	5.45	1.33	2.69
10	0.78	−0.79	−6.46	9.21	2.61	4.80
50	1.20	−1.18	−4.89	7.21	1.83	3.83
100	1.15	−1.16	−4.69	7.28	1.91	4.18

Most of the flooded area is within or shallower than the depth class of 1.2 m, but it should be noted that even a flood depth of 1 m can cause extensive damage to urban areas and therefore, the downstream area must be considered to be at high risk of floods. This research work has endeavored to classify the depths of the floods in Koraiyar River basin during the occurrence of extreme rainfall and the severity of flood hazard to the people residing near the river basin.

After generating the floodplain map, the liabilities of different land use types and settlements are identified, representing the first step towards comprehensive flood hazard mapping.

Weight allocation for flood hazard map preparation

In the Koraiyar basin, the maps are prepared after digitizing and plotting the rank factor assigned for each selected parameter. The maximum flood flow, slope, and settlement density are taken as rank factors, and the weights are assigned for the basin, as shown in Table 7. The weightage is assigned based on suggestions by Public Works Department Engineers, Hydrologists and Flood Experts. Each factor is allocated for different classes, and each class is assigned weights based upon the parameters that are likely to cause floods. The calculated weights are inputted in raster calculator in ArcGIS in spatial analyst extension. The raster calculator is used to estimate the probability of flood occurrence, and the total weights are considered by assigning the re-class raster for each factor responsible for a chance of occurrence of flooding.

Delineation of flood hazard maps

For efficient flood forecasting and reliable warning, flood hazard maps are required in the initial stages of urban developmental activities in the basin. The flood hazard maps in this study are generated for a chosen extreme rainfall event in the Koraiyar basin for various LULC changes between 1986 and 2036. The maps obtained show that the flood hazard of the basin increases between the years 1986 and 2036. In this study, the flood hazard maps of maximum flood extent for different return periods are prepared from the maximum flood flow, slope, and settlement density of the basin by using ArcGIS software 10.2.2 to generate flood hazard maps.

Table 7 Rank of the factor and Raster re-class (weighted) factor for the study area

Factors	Rank
Flood flow	3
Basin slope	2
Settlements	1

The flood hazard maps are prepared in the raster format to generate the flood depth for various return periods. The generated raster formats are converted into vector format, and the extreme flood spread area polygons are clipped for the different return periods for different LULC conditions. The clipped raster maps are made uniform by using the slice tool in ArcGIS. From the allocated weights, the flood hazard map is categorized into seven classes, namely (no flood hazard, very very low, very low, low, moderate, high, and very high) by the standard deviation method of classification. The classwise susceptibility areas of flood hazard for different LULC of the years 1986–2036 are shown in Table 8.

The results obtained for the LULC conditions of the year 1986, depicted in Fig. 10, show that the flood hazard area falls under very high hazard class and is 192.26 km² of the whole basin. The Koraiyar River basin has a high hazard area of 485.72 km² followed by moderate, low, very low, and very very low hazard areas of the basin. The total flood hazard area spread across the basin during this year is 819.13 km². Due to LULC condition in the year 1996, there is a higher flood hazard area of 234.53 km² compared with very high hazard class, as shown in Fig. S6. During this year, it is noted that the basin experienced a very very low hazard area of 13.14 km² of the whole area of the basin. The overall flood hazard area of the basin during this year is observed to be 571.24 km². The reduction of the flood hazard is noticed because of soil characteristics and an

increase in open space in the basin. From Fig. S7, it is clear that in the year 2006, there is still lower value of flood hazard area due to geographic factors and additional drainage facilities in the basin. An increase in the flood hazard area from 571.24 to 780.15 km² is noted during the year 2016, as seen in Fig. 11. This is mostly due to the increased urbanization in the basin. The predicted flood hazard map for the LULC change in the year 2026 shown in Fig. S8 is based on land use, impervious nature of the basin and submerged areas based upon flood depth; the map shows an increase in flood hazard area to 835.84 km². For the simulated year of 2036, the northern part of sub-basins located in Tiruchirappalli city falls under very high and high hazard area followed by medium hazard area, as seen in Fig. 12. The year 2036 is observed to have a greater extent of flood hazard area than in 2026 with a hazard area of 845.68 km².

From the results, it is evident that the flood hazard extent has increased by 4.32% in the high hazard zones from 1986 to 2036, as shown in Table 9. The very high hazard zone during this period is 3.65% in the Koraiyar basin. It is perceived that the very low hazard zone occupies more area in the basin in the present and future prediction of flood hazard maps. According to Sahoo and Sreeja (2016), urban flooding is significantly different from rural flooding as urbanization leads to a 1.8 to 8 times increase in the flood peaks and up to 6 times increase in the flood volumes. Therefore, from the analysis, it is observed that increase in imperviousness and settlement areas in the basin increases the maximum hazard area in the basin.

The following observations are noted the flood hazard study:

1. Even though the extreme rainfall remains the same for the study period of 1986–2036 despite changing

Table 8 Flood hazard areas for different LULC and return periods

S. no	Classification of the flood	Flood hazard area (km ²)					
		LULC 1986	LULC 1996	LULC 2006	LULC 2016	LULC 2026	LULC 2036
1	Very very low	13.63	13.14	13.63	12.69	13.65	13.75
2	Very low	22.21	22.64	22.21	21.00	22.45	22.68
3	Low	29.58	30.47	29.58	27.72	30.64	31.42
4	Moderate	75.73	77.40	75.72	73.00	77.25	78.49
5	High	485.72	234.53	485.56	461.78	496.83	500.49
6	Very high	192.26	193.06	192.19	183.96	195.02	198.85

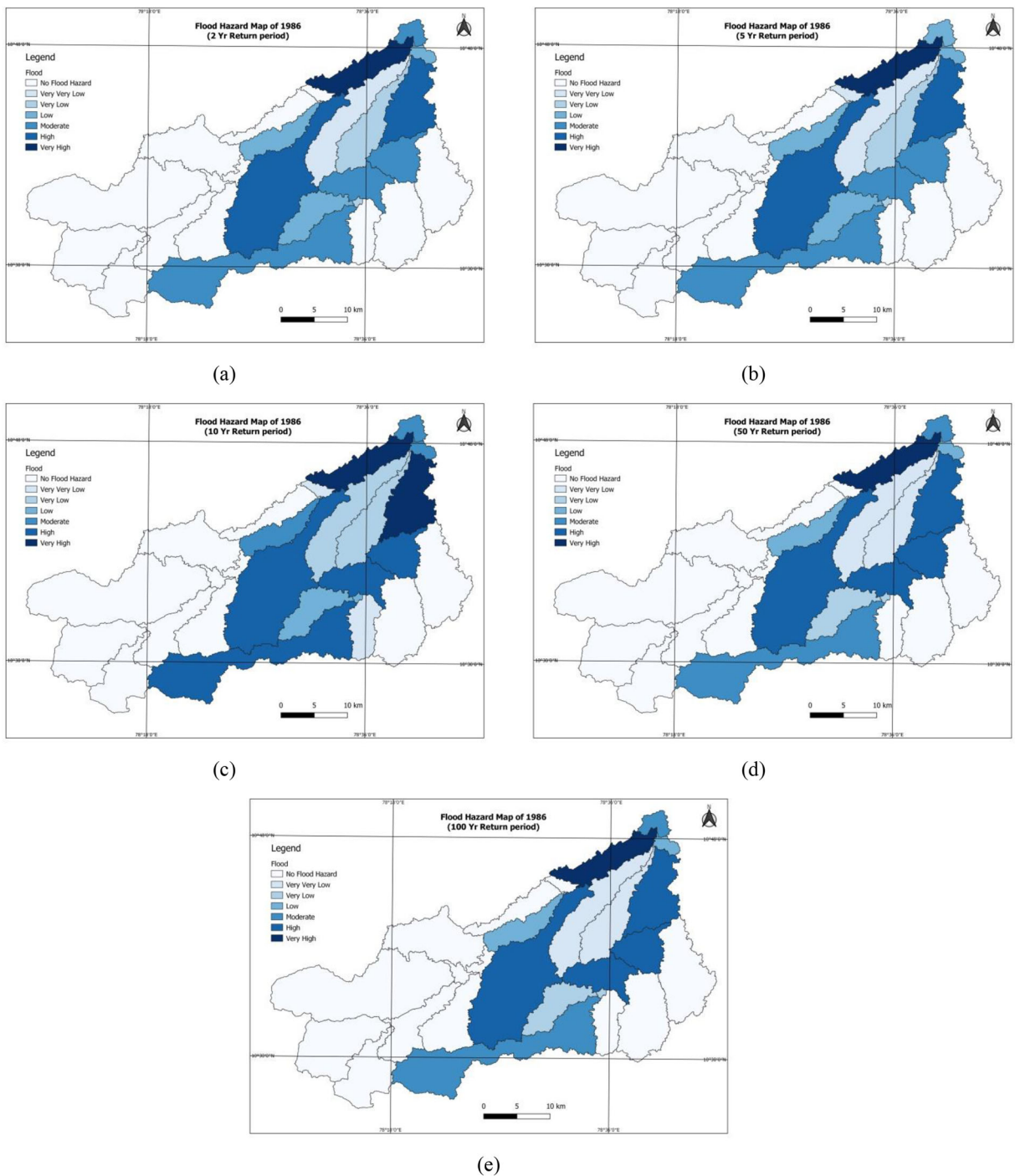


Fig. 10 Developed flood hazard map of the year 1986 for different return periods: **a** 2, **b** 5, **c** 10, **d** 50, and **e** 100

- land use, the flood depth and hazard area are observed to increase with time.
- The increase in flood depth is mostly due to the presence of flat terrain throughout the basin.
- The central portion of the basin is vulnerable to very high flood hazard throughout the study period.
- From the hazard map, it is observed that the northern area of the basin in Tiruchirappalli city is highly

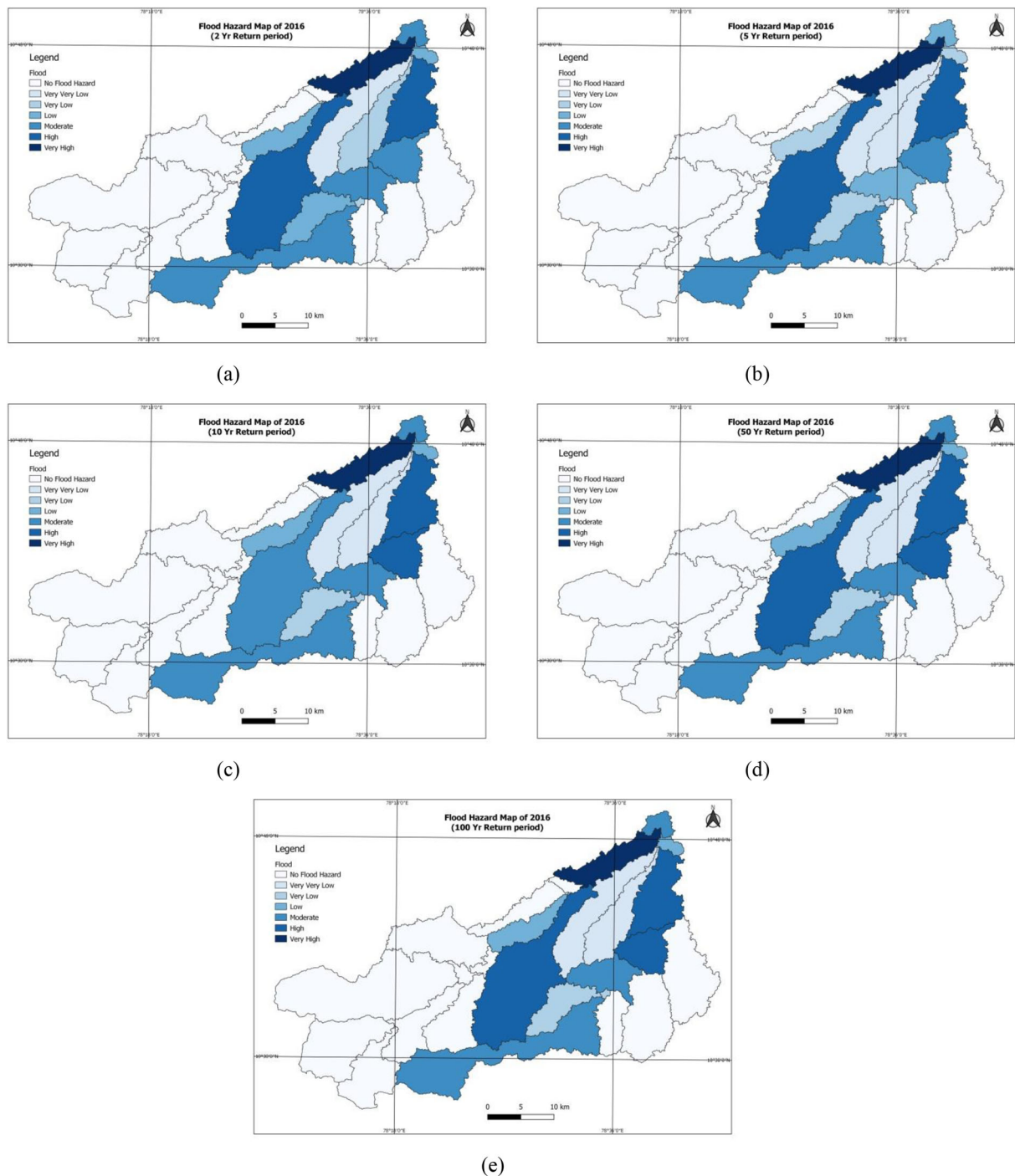


Fig. 11 Developed flood hazard map of the year 2016 for different return periods: **a** 2, **b** 5, **c** 10, **d** 50, and **e** 100

vulnerable to flood hazard due to rapid land use changes.

5. The study shows that the flood hazard increases from 1986 to 2036 due to LULC changes occurring

in the Koraiyar basin, a finding which is in agreement with previous studies (Miller et al. 2014; Zope et al. 2015; Sahoo and Sreeja 2016; Sahoo and Sreeja 2018) which observed that the flood risk increases with urban growth and land use changes.

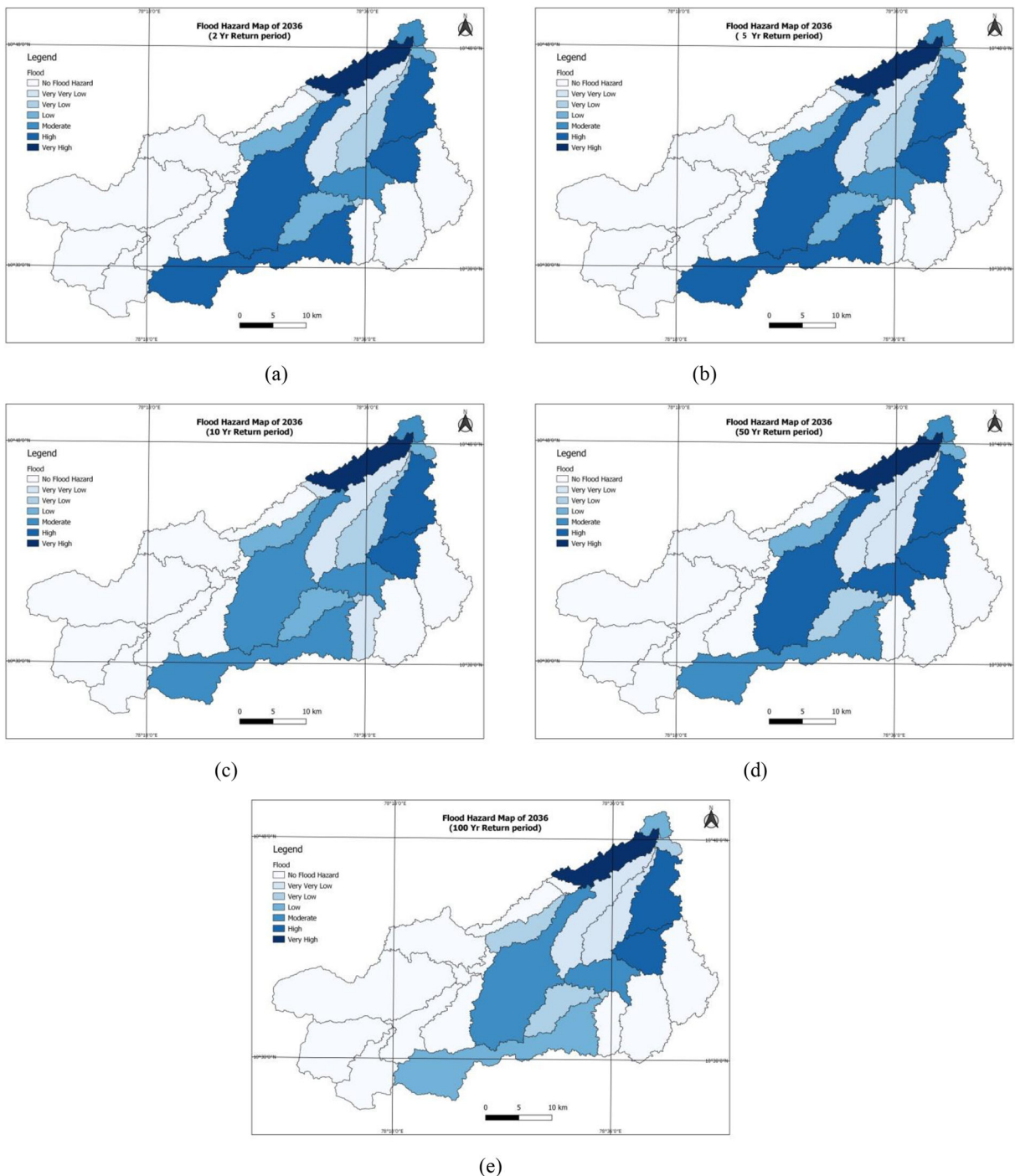


Fig. 12 Simulated flood hazard maps for the future year of 2036 for various return periods: **a** 2, **b** 5, **c** 10, **d** 50, and **e** 100

The predicted flood hazard map shows that there are not many changes in flood spread hazard with respect to LULC conditions except for the flood depth. The projected flood hazard maps prepared for this basin are useful for drawing up early flood

warning and mitigation measures in vulnerable land sections. The flood hazard maps are also beneficial for other purposes like flood insurance and in the identification of flood threat due to extreme rainfall in the basin.

Table 9 Percentage of difference in flood hazard area for different LULC and return periods

S. no	Classification of the flood	Flood hazard area (%)					
		1986–1996	1996–2006	2006–2016	2016–2026	2026–2036	1986–2036
1	Very very low	− 7.14	7.69	− 7.14	7.69	0.00	0.00
2	Very low	4.55	− 4.35	− 4.55	4.76	4.55	4.55
3	Low	0.00	0.00	− 6.67	10.71	0.00	3.33
4	Moderate	1.32	− 1.30	− 3.95	5.48	1.30	2.63
5	High	− 51.65	1.28	94.12	7.58	2.01	4.32
6	Very high	0.52	− 0.52	− 4.17	5.98	2.05	3.65

Conclusions

In this study, the LULC changes and their effect on flood flow in the Koraiyar River basin have been studied. The floodplain and flood hazard maps for the basin are prepared by considering parameters such as flood depth and land use. The present study deals with the methodology for generating floodplain and hazard maps for the Koraiyar basin through HEC-GeoRAS processing. The basin boundary and the runoff of the basin are derived using HEC GeoHMS process. In the current study, the influence of LULC change and the effect of urbanization on flooding are studied for the Koraiyar basin by considering the LULC changes for the present years (1986–2016) as well as for the future years (2026–2036). The integrated approach of hydrologic and hydraulic models of HEC-HMS, HEC-GeoHMS, HEC-RAS, HEC-GeoRAS along with GIS and remote sensing is adapted for generating the rainfall-runoff and flood maps for the river basin. The LULC analysis of the basin shows that there is 1.4% increase in the settlement area of the whole basin leading to a 3% increase in runoff rate of the basin. The analysis of LULC changes shows that there is only marginal increase in settlement areas and open lands. Consequently, there is only marginal increase in the volume of surface runoff in the basin.

The following conclusions are made based on the obtained results:

1. The worst-affected area is the northern part of the basin where the flood depth reached up to 4.7 m.
2. Tiruchirappalli city, located in the central part of the basin, is also observed to be a high flood hazard zone, and the flood hazard is found to increase with

an increase in imperviousness following escalating urban development.

3. The flood hazard maps show that a maximum of 819.23 to 845.68 km² of the basin area is classified as being susceptible to floods, which is almost 51.96% of the basin.
4. From the study, it is also observed that the very low hazard zone occupies more area in the basin in the present and the future predictions of flood hazard maps.

Merits of the study:

1. The modeling method adopted in this study has precisely identified the possible critical flood events.
2. The model developed has successfully adopted a reliable approach even with limited availability of data on the river basin and it can be used in a similar manner for other ungauged basins.
3. It is also proved that the model is an accessible tool for real-time preventive solutions and when immediate actions need to be implemented before a flood crisis.

The recommendations of the study:

The flood risk map developed in the basin can be effectively used for improving public awareness of flood threat, by giving the public early warning with the help of accurate and reliable flood forecasting systems. The maps developed in this study can be used by the Tiruchirappalli City Corporation for early flood warning measures; it can also serve as a valuable tool for appropriate disaster preparedness and flood mitigation measures. The evacuation maps and safe shelters can be identified and planned by using such hazard

maps. The developed flood risk and inundation maps can be effectively used for future planning and developmental work in the Koraiyar River basin.

Further scope of the study:

In the future, floodplain analysis should be done with better topographical and hydrological data by working with river bathymetry, Lidar surveys, and Differential Global Positioning System (DGPS) surveys across the river basin. Such spatial studies will provide more or less acceptable scenarios in identification of floodplain and flood hazard areas in the Koraiyar basin. Thereby, effective precautionary measures against future flood events can be taken.

Acknowledgments The authors extend their sincere gratitude to the US Army Corps of Engineers for providing HEC-HMS and HEC-RAS as open-source software. The authors also acknowledge the assistance of the State Surface And Groundwater Data Centre, Chennai in providing access to rainfall data. They are also thankful to the editorial board and anonymous reviewers for providing their constructive comments, which have helped to improve the manuscript. The authors also extend their grateful thanks to USACE for providing open-source software free of charge and ALOS for providing DEM data.

Compliance with ethical standards

Conflict of interest The authors declare that they have no conflict of interest.

References

Abdel-Fattah, M., Saber, M., Kantoush, S., Khalil, F., & Sumi, T. S. A. (2017). A hydrological and geomorphometric approach to understanding the generation of wadi flash foods. *Water, 9*, 553. <https://doi.org/10.3390/w9070553>.

Acosta-Coll, M., Ballester-Merelo, F., & Marcos Marti'nez-Peiro'. (2018). Early warning system for detection of urban pluvial flooding hazard levels in an ungauged basin. *Natural Hazards, 92*, 1237–1265.

Alfieri, L., Salamon, P., Bianchi, A., Neal, J., Bates, P., & Feyen, L. (2014). Advances in pan-European flood hazard mapping. *Hydrological Processes, 28*(13), 4067–4077.

Alley, R. B., Marotzke, J., Nordhaus, W. D., Overpeck, J. T., Petet, D. M., Pielke RA Jr, Pierrehumbert, R. T., Rhines, P. B., Stocker, T. F., Talley, L. D., & Wallace, J. M. (2003). Abrupt climate change. *Science, 299*, 2005–2010.

An Thi Ngoc Dang, & Lalit Kumar. (2017). Application of remote sensing and GIS-based hydrological modelling for flood risk analysis: a case study of District 8, Ho Chi Minh city,

Vietnam. *Geomatics, Natural Hazards and Risk, 8*(2), 1792–1811.

Arnold, J. G., Srinivasan, R., Mutiah, R. S., & Williams, J. R. (1998). Large area hydrologic modeling and assessment—part 1: model development. *Journal of the American Water Resources Association, 34*, 73–89. <https://doi.org/10.1111/j.1752-1688.1998.tb05961.X>.

Aryal, et al. (2020). A model-based flood hazard mapping on the southern slope of Himalaya. *Water, 12*, 540. <https://doi.org/10.3390/w12020540>.

Ashmore, P., & Church, M. (2001). The impact of climate change on rivers and river processes in Canada. *Geological Survey of Canada, 555*, 58.

Bharath, R., & Elshorbagy, A. (2018). Flood mapping under uncertainty: a case study in the Canadian prairies. *Natural Hazards, 94*, 537–560. <https://doi.org/10.1007/s11069-018-3401-1>.

Bhuiyan, M. A., Kumamoto, T., & Suzuki, S. (2015). Application of remote sensing and GIS for evaluation of the recent morphological characteristics of the lower Brahmaputra-Jamuna River, Bangladesh. *Earth Science Informatics, 8*(3), 551–568.

Changnon, S. A., Pielke, R. A., Changnon, D., Sylves, R. T., & Pulwarty, R. (2000). Human factors explain the increased losses from weather and climate extremes. *Bulletin of the American Meteorological Society, 81*(3), 437–442.

Chen, J., Hill, A. A., & Urbano, L. D. (2009a). A GIS-based model for urban flood inundation. *Journal of Hydrology, 373*(1), 184–192.

Chen, Y., Xu, Y., & Yin, Y. (2009b). Impacts of land use change scenarios on storm-runoff generation in Xitiaoqi basin, China. *Quaternary International, 208*, 121–128. <https://doi.org/10.1016/j.quaint.2008.12.014>.

Cheng, L., Agakouchak, A., Gilleland, E., & Katz, R. W. (2014). Non-stationary extreme value analysis in changing climate. *Climate Change, 127*, 353–369.

Chow, V. T. (1959). *Open channel hydraulics* (pp. 3–127). Inc, New York: McGraw-Hill Book Company.

Chow, V. T., Maidment, D. R., & Mays, L. W. (1988). *Applied hydrology*. New York: McGraw-Hill.

Costae, M. H., Botta, A., & Cardille, J. A. (2003). Effects of large-scale changes in land cover on the discharge of the Tocantins river, Southeastern Amazonia. *Journal of Hydrology, 283*(1–4), 206–217.

Daniel, C., & Mays, L. W. (2015). Development of an optimization/simulation model for real-time flood-control operation of river-reservoirs systems. *Water Resources Management, 29*, 3987–4005. <https://doi.org/10.1007/s11269-015-1041-8>.

Derdour, A., & Bouanani, A. (2019). Coupling HEC-RAS and HEC-HMS in rainfall–runoff modeling and evaluating floodplain inundation maps in arid environments: case study of Ain Sefra city, Ksour Mountain, SW of Algeria. *Environmental Earth Sciences, 78*, 586. <https://doi.org/10.1007/s12665-019-8604-6>.

Derdour, A., Bouanani, A., & Baba-Hamed, K. (2017). Hydrological modeling in semi-arid region using HEC-HMS model. Case study in Ain Sefra watershed, Ksour Mountains (SW, Algeria). *Journal of Fundamental and Applied Sciences, 92*, 1027–1049. <https://doi.org/10.4314/jfas.v9i2.27>.

- Dewan, A. M., & Yamaguchi, Y. (2009). Land use and land cover change in Greater Dhaka, Bangladesh: using remote sensing to promote sustainable urbanization. *Applied Geography*, *29*, 390–401.
- Dewan, A. M., Kumamoto, T., & Nishigaki, M. (2006). Flood hazard delineation in Greater Dhaka, Bangladesh using an integrated GIS and remote sensing approach. *Geocarto International*, *21*(2), 33–38. <https://doi.org/10.1080/10106040608542381>.
- Dhruvesh, P. P., Ramirez, J. A., Srivastava, P. K., Bray, M., & Han, D. (2017). Assessment of flood inundation mapping of Surat city by coupled 1D/2D hydrodynamic modeling: a case application of the new HEC-RAS 5. *Natural Hazards*, *89*, 93–130. <https://doi.org/10.1007/s11069-017-2956-6>.
- European Parliament Council (2007) Directive 2007/60/EC of the European Parliament and of the Council of 23 October 2007 on the assessment and management of flood risks. <https://eur-lex.europa.eu/legal-content/EN/TXT/?uri=celex:52007SC1416>.
- Gallegos, H. A., Schubert, J. E., & Sanders, B. F. (2009). Two-dimensional, high-resolution modeling of urban dam-break flooding: a case study of Baldwin Hills, California. *Advances in Water Resources*, *32*, 1323–1335.
- Gao, W., Shen, Q., Zhou, Y., & Li, X. (2018). Analysis of flood inundation in ungauged basins based on multi-source remote sensing data. *Environmental Monitoring and Assessment*, *190*, 129.
- Gaume, E., Bain, V., Bernardara, P., Newinger, O., Barbuc, M., Bateman, A., Blaškovičová, L., Blöschl, G., Borga, M., Dumitrescu, A., Daliakopoulos, I., Garcia, J., Irimescu, A., Kohnova, S., Koutroulis, A., Marchi, L., Matreata, S., Medina, V., Preciso, E., Sempere-Torres, D., Stancalie, G., Szolgyai, J., Tsanis, I., Velasco, D., & Viglione, A. (2009). A compilation of data on European flash floods. *Journal of Hydrology*, *367*, 70–78.
- Ghanbarpour, M. R., Mohsen, M., & Saravi, S. S. (2014). Floodplain inundation analysis combined with contingent valuation: implications for sustainable flood risk management. *Water Resources Management*, *28*, 2491–2505.
- Guhasapir, D., Hargitt, D., Hoyois, P. (2004) Thirty Years of Natural Disasters 1974–2003: The Numbers. Presses 728 universitaires de Louvain- Belgium, Brussels, p 188.
- Hajat, S., Ebi, K. L., Kovats, S., Menne, B., Edwards, S., & Haines, A. (2003). The human health consequences of flooding in Europe and the implications for public health. *Applied Environmental Science and Public Health*, *1*(1), 13–21.
- Hassan, M. A., Church, M., Lisle, T. E., Brardinoni, F., Benda, L., & Grant, G. E. (2005). Sediment transport and channel morphology of small, forested streams. *Journal of the American Water Resources Association*, *41*(4), 853–876.
- Hathout, S. (2002). The use of GIS for monitoring and predicting urban growth in East and West St Paul, Winnipeg, Manitoba, Canada. *Journal of Environmental Management*, *66*, 229–238.
- HEC-RAS, reference manual (2016) USACE, version 5.0. US Army Corps of Engineers, CPD-68.
- Herold, M., Goldstein, N. C., & Clarke, K. C. (2003). The spatio-temporal form of urban growth: measurement, analysis and modeling. *Remote Sensing of Environment*, *86*, 286–302.
- Jan Klimes, Miroslava Benes'ova', Vi't Vil'mek, Petr Bous'ka, & Alejo Cochachin Rapre. (2014). The reconstruction of a glacial lake outburst flood using HEC-RAS and its significance for future hazard assessments: an example from Lake 513 in the Cordillera Blanca, Peru. *Natural Hazards*, *71*, 1617–1638. <https://doi.org/10.1007/s11069-013-0968-4>.
- Jayaraman, V., Chandrasekhar, M. G., & Rao, U. R. (1997). Managing the natural disasters from space technology inputs. *Acta Astronautica*, *40*(2–8), 291–325.
- Jonkman, S. N., & Kelman, I. (2005). An analysis of causes and circumstances of flood disaster deaths. *Disasters*, *29*(1), 75–97.
- Karagiorgos, K., Thaler, T., Heiser, M., Hübl, J., & Fuchs, S. (2016). Integrated flash food vulnerability assessment: insights from East Attica, Greece. *Journal of Hydrology*, *541*(A), 553–562. <https://doi.org/10.1016/j.jhydrol.2016.02.052>.
- Karbasi, M., Shokoohi, A., & Saghafian, B. (2018). Loss of life estimation due to flash floods in residential areas using a regional model. *Water Resources Management*, *32*, 4575–4589. <https://doi.org/10.1007/s11269-018-2071-9>.
- Kleinhans, M. G. (2005). Flow discharge and sediment transport models for estimating a minimum timescale of hydrological activity and channel and delta formation on Mars. *Journal of Geophysical Research*, *110*, E12003. <https://doi.org/10.1029/2005JE002521>.
- Koneti, S., & Sri lakshmi, S., Parth sarathi, R. (2018). Hydrological Modeling with Respect to Impact of Land-Use and Land-Cover Change on the Runoff Dynamics in Godavari River Basin Using the HEC-HMS Model. *International Journal of Geo-Information*, *7*, 206. <https://doi.org/10.3390/ijgi7060206>
- Kwan Tun Lee, & Pin-Chun Huang. (2018). Assessment of flood mitigation through riparian detention in response to a changing climate—a case study. *Journal of Earth System Science*, *127*, 83. <https://doi.org/10.1007/s12040-018-0983-7>.
- Lambin, E. F., Geist, H., & Lepers, E. (2003). Dynamics of land use and cover change in tropical regions. *Annual Review of Environment and Resources*, *28*, 205–241.
- Lugeri, N., Kundzewicz, Z. W., Genovese, E., Hochrainer, S., & Radziejewski, M. (2010). River flood risk and adaptation in Europe—assessment of the present status. *Mitigation and Adaptation Strategies for Global Change*, *15*, 621–639.
- Madadi, M. R., Azamathulla, H. M., & Yakhkeshi, M. (2015). Application of Google earth to investigate the change of flood inundation area due to flood detention dam. *Earth Science Informatics*, *8*, 627–638. <https://doi.org/10.1007/s12145-014-0197-8>.
- Mai, D. T., & Smedt, F. D. (2017). A combined hydrological and hydraulic model for flood prediction in Vietnam applied to the Huong River basin as a test case study. *Water*, *9*, 879. <https://doi.org/10.3390/w9110879>.
- Mallikarjun, M., Vikas, D., Prudhviraju, K. N., Patel, S. B., & Mohan, K. (2019). Precision mapping of boundaries of flood plain river basins using high-resolution satellite imagery: a case study of the Varuna river basin in Uttar Pradesh, India. *Journal of Earth System Science*, *128*, 105. <https://doi.org/10.1007/s12040-019-1146-1>.
- Masood, M., & Takeuchi, K. (2012). Assessment of flood hazard, vulnerability and risk of mid-eastern Dhaka using DEM and 1D hydrodynamic model. *Natural Hazards*, *61*(2), 757–770.

- Melesse, A. M., & Shih, S. F. (2002). Spatially distributed storm runoff depth estimation using Landsat images and GIS. *Computers and Electronics in Agriculture*, 37, 173–183.
- Merritt, W.S., Letcher, R.A., Jakeman, A.J. (2003). A review of erosion and sediment transport models. *Environ Model Softw*, 18(8), 761–799.
- Merwade, V., Cook, A., & Coonrod, J. (2008). GIS techniques for creating river terrain models for hydrodynamic modeling and flood inundation mapping. *Environmental Modelling and Software*, 23, 1300–1311.
- Miller, J. D., Kim, H., Kjeldsen, T. R., Packman, J., Grebby, S., & Dearden, R. (2014). Assessing the impact of urbanization on storm runoff in a peri-urban catchment using historical change in impervious cover. *Journal of Hydrology*, 515, 59–70.
- Moriassi, D. N., Arnold, J. G., Van Liew, M. W., Bingner, R. L., Harmel, R. D., & Veith, T. L. (2007). Model evaluation guidelines for systematic quantification of accuracy in watershed simulations. *American Society of Agricultural and Biological Engineers*, 50(3), 885–900.
- Neeraj, K. D. L., Arpan, S., & Issac, R. K. (2017). Applicability of HEC-RAS & GFMS tool for 1D water surface elevation/flood modeling of the river: a case study of River Yamuna at Allahabad (Sangam), India. *Modeling Earth Systems and Environment*. <https://doi.org/10.1007/s40808-017-0390-0>.
- Nikolakopoulos, K. G., Choussiafis, C., & Karathanassi, V. (2015). Assessing the quality of DSM from ALOS optical and radar data for automatic drainage extraction. *Earth Science Informatics*, 8, 293–307. <https://doi.org/10.1007/s12145-014-0199-6>.
- Parry, M.L., Canziani, O.F., Palutikof, J.P., vanderlinden, P.J., Hanson, C.E. (2007). Summary for policymakers in: Climate change 2007: impacts, adaptation and vulnerability. Contribution of working group II to the fourth assessment report of the intergovernmental panel on climate change. (pp.7–22). Cambridge University Press, Cambridge.
- Prama, M., Omran, A., Schröder, D., & Abouelmagd, A. (2020). Vulnerability assessment of fish foods in Wadi Dahab Basin. *Egypt Journal of Remote Sensing*, 79, 114. <https://doi.org/10.1007/s12665-020-8860-5>.
- Price, R. K., & Vojinovic, Z. (2008). Urban flood disaster management. *Urban Water Journal*, 5(3), 259–276.
- Quiroga, V. M., Kure, S., Udo, K., & Mano, A. (2016). Application of 2D numerical simulation for the analysis of the February 2014 Bolivian Amazonia flood: application of the new HEC-RAS version 5. *RIBAGUAREvista Iberoamericana del Agua*, 3, 25–33.
- Rajeevan, M., & Bhate, J. (2008). A high resolution daily gridded rainfall data set (1971–2005) for mesoscale meteorological studies, *NCC Research Report, No.9*. Indian Meteorological Department.
- Sahoo, S. N., & Sreeja, P. (2014). A methodology for determining runoff based on imperviousness in an ungauged Peri urban catchment. *Urban Water Journal*, 11(1), 42–54.
- Sahoo, S. N., & Sreeja, P. (2015). Development of Flood Inundation Maps and Quantification of Flood Risk in an Urban Catchment of Brahmaputra River. *ASCE-ASME Journal of Risk and Uncertainty in Engineering Systems, Part A: Civil Engineering*, 3(1), A4015001. <https://doi.org/10.1061/ajrua6.00>
- Sahoo, S. N., & Sreeja, P. (2016). Determination of effective impervious area for an urban Indian catchment. *Journal of Hydrologic Engineering*. [https://doi.org/10.1061/\(ASCE\)HE.1943-5584.0001346](https://doi.org/10.1061/(ASCE)HE.1943-5584.0001346), 05016004-1–05016004-10.
- Sahoo, S. N., & Sreeja, P. (2018). Detention ponds for managing flood risk due to increased imperviousness: case study in an urbanizing catchment of India. *Natural Hazards Review*, 19(1), 05017008. [https://doi.org/10.1061/\(ASCE\)NH.1527-6996.0000271](https://doi.org/10.1061/(ASCE)NH.1527-6996.0000271)
- Salimi, S., Ghanbarpour, M. R., Solaimani, K., & Ahmadi, M. Z. (2008). Floodplain mapping using hydraulic simulation model in GIS. *Journal of Applied Sciences*, 8, 660–665.
- Sarhadi, A., Soltani, S., & Modarres, R. (2012). Probabilistic flood inundation mapping of ungauged rivers: linking GIS techniques and frequency analysis. *Journal of Hydrology*, 458, 68–86.
- Serra, P., Pons, X., & Sauri, D. (2008). Land-cover and land-use change in a Mediterranean landscape: a spatial analysis of driving forces integrating biophysical and human factors. *Applied Geography*, 28, 189–209.
- Siart, C., Bubenzer, O., & Eitel, B. (2009). Combining digital elevation data (SRTM/ASTER), high resolution satellite imagery (Quickbird) and GIS for geomorphological mapping: a multi-component case study on Mediterranean karst in Central Crete. *Geomorphology*, 112, 106–121.
- Smith, L. C. (1997). Satellite remote sensing of river inundation area, stage, and discharge: a review. *Hydrological Processes*, 11, 1427–1439.
- Stevens, M. R., & Hanschka, S. (2014). Municipal flood hazard mapping: the case of British Columbia, Canada. *Natural Hazards*, 73(2), 907–932.
- Sunkpho, J., & Ootamakom, C. H. (2011). Real-time flood monitoring and warning system. Songklanakarinn. *Journal of Science and Technology*, 33(2), 227–235.
- Surendar, N., & Nisha, R. (2019a). Estimation of flood mitigation parameter for Tiruchirappalli city using mathematical relational model. *Indian Journal of Geo Marine Sciences*, 49(07), 1269–1279.
- Surendar, N., & Nisha, R. (2019b). Simulation of extreme event-based rainfall-runoff process of an urban catchment area using HEC-HMS. *Modeling Earth Systems and Environment*, 5, 1867–1881. <https://doi.org/10.1007/s40808-019-00644-5>.
- Tarboton, D. G., & Ames, D. P. (2001). Advances in the mapping of flow-networks from digital elevation data. In *Proceedings of the World Water And Environmental Resources Congress: may 20–24*. Florida: American Society of Civil Engineers.
- Thirumurugan, P., & Krishnaneni, M. (2018). Flood hazard mapping using geospatial techniques and satellite images—a case study of coastal district of Tamil Nadu. *Environmental Monitoring and Assessment*, 191, 193. <https://doi.org/10.1007/s10661-019-7327-1>.
- Thomas, R. F., Kingsford, R. T., Lu, Y., Cox, S. J., Sims, N. C., & Hunter, S. J. (2015). Mapping inundation in the heterogeneous floodplain wetlands of the Macquarie marshes, using Landsat thematic mapper. *Journal of Hydrology*, 524, 194–213. <https://doi.org/10.1016/j.jhydrol.2015.02.029>.
- UCAR (University Corporation for Atmospheric Research) (2010). Flash flood early warning system reference guide 2010. ISBN 978-0-615-37421-5.

- Verma, A. K., Jha, M. K., & Mahana, R. K. (2010). Evaluation of HEC-HMS and WEPP for simulating watershed runoff using remote sensing and geographical information system. *Paddy and Water Environment*, 8, 131–144. <https://doi.org/10.1007/s10333-009-0192-8>.
- Ward, R. (1978). *Floods: a geographical perspective*. London: MacMillan.
- Weaver, A. (2016). Reanalysis of flood of record using HEC-2, HEC-RAS, and USGS gauge data. *Journal of Hydrologic Engineering*, 21(6), 05016011. [https://doi.org/10.1061/\(ASCE\)HE.1943-5584.0001354](https://doi.org/10.1061/(ASCE)HE.1943-5584.0001354).
- Wheater, H. S., Jolley, T. J., Onof, C., Mackay, N., & Chandler, R. E. (1999). Analysis of aggregation and disaggregation effects for grid-based hydrological models and the development of improved precipitation disaggregation procedures for GCMs. *Hydrology and Earth System Sciences*, 3, 95–108. <https://doi.org/10.5194/hess-3-95-1999>.
- Wu, W., Shields, F. D., Bennett, S. J., & Wang, S. S. (2005). A depth-averaged two dimensional model for flow, sediment transport, and bed topography in curved channels with riparian vegetation. *Water Resources Research*, 41, W03015. <https://doi.org/10.1029/2004WR003730>.
- Yang, J., Townsend, R. D., & Daneshfar, B. (2006). Applying the HEC-RAS model and GIS techniques in river network floodplain delineation. *Canadian Journal of Civil Engineering*, 33, 19–28. <https://doi.org/10.1139/L05-102>.
- Younghun, J., Dongkyun, K., Dongwook, K., Munmo, K., Seung, O.L. (2014). Simplified flood inundation mapping based on flood elevation-discharge rating curves using satellite images in gauged watersheds. *Water*, 6, 1280–1299. <https://doi.org/10.3390/w6051280>.
- Yu, W., Nakakita, E., Kim, S., & Yamaguchi, K. (2015). Improvement of rainfall and flood forecasts by blending ensemble NWP rainfall with radar prediction considering orographic rainfall. *J Hydrol*, 531(part 2), 494–507. <https://doi.org/10.1016/j.jhydrol.2015.04.055>.
- Zaharia, L., Costache, R., Remus Pr av'alie, & Minea, G. (2015). *Journal of Earth System Science*, 124(6), 1311–1324.
- Zhang, X.S., Srinivasan, R., Debele, B., Hao, F.H. (2008). Runoff simulation of the headwaters of the Yellow River using the SWAT model with three snowmelt algorithms. *Journal of the American Water Research Association*, 44, 48–61. <https://doi.org/10.1111/j.1752-1688.2007.00137.x>.
- Zhang, W., Yanhong, X., Yanru, W., & Hong, P. (2014). Modeling sediment transport and river bed evolution in river system. *Journal of Clean Energy Technologies*, 2, 175–179. <https://doi.org/10.7763/jocet.2014.v2.117>.
- Zope, P. E., Eldho, T. I., & Jothiprakash, V. (2015). Impacts of urbanization on flooding of a coastal urban catchment: a case study of Mumbai City, India. *Natural Hazards*, 75, 887–908.
- Zope, P. E., Eldho, T. I., & Jothiprakash, V. (2016). Impacts of land use–land cover change and urbanization on flooding: a case study of Oshiwara River basin in Mumbai, India. *Catena*, 145, 142–154.

Publisher's note Springer Nature remains neutral with regard to jurisdictional claims in published maps and institutional affiliations.